REGULATION OF CANCER STEM CELL FUNCTIONS BY ACTIN FILAMENT DYNAMICS

by
Vesselin Ruslanov Penchev

A dissertation submitted to Johns Hopkins University in conformity with the requirements for the degree of Doctor of Philosophy

Baltimore, Maryland
March, 2016

Abstract

Cancer stem cells (CSCs) have been identified in a multitude of malignancies as an important regulator of tumor self-renewal and disease progression, and relapse. Their functions indicate that targeting of CSCs will improve clinical outcomes. Multiple phenotypic CSC populations have been isolated within the same disease, and their precise relationship is unclear. Using pancreatic cancer as a model we demonstrate plasticity where non-overlapping CSC populations give rise to each other. Surprisingly our results also indicate that non-CSCs could potentially give rise to CSCs. Thus, mechanisms that are fundamental to the maintenance of CSCs need to be identified, since successful therapeutic strategies should target all sources of self-renewal within the tumor. We identify modulation of actin filament dynamics as a novel mechanism for the regulation of CSC functions. Pancreatic CSCs are characterized by a low polymerized to free actin ratio relative to the bulk of the tumor. Inducing actin polymerization decreases CSC frequency and leads to the loss of self-renewal, and migratory capacity in vitro and a marked decrease of in vivo tumorigenicity. Targeting actin dynamics decreases the frequency of three phenotypic CSC populations, suggesting that modulation of actin organization could be a fundamental mechanism for CSC regulation. Modulators of actin dynamics specifically overexpressed in cancers can be utilized as therapeutic targets, and we used pharmacological inhibition of the cytoskeletal modulator Ezrin to decrease the tumorigenicity of human derived samples. Our work demonstrates that investigating mechanisms of actin regulation in cancers could lead to the development of better strategies to target CSC, and therefore improve clinical outcomes.

Acknowledgements

I would like to thank my mentor Dr. William Matsui for all of his support throughout my journey. I have never met someone who cares so much about the growth of his students. His drive and kindness are inspiring and hope I will be able to repay all the time and energy he devoted to my success.

I would also like to thanks Dr. Zeshaan Rasheed, who introduced me to the lab and took on the day-to-day mentoring duties. His friendship and positive outlook have kept me going on many occasions.

I would like to thank Dr. Aykut Uren and Dr. Jim Eshleman for all their advice and help throughout the years.

I would also like to thank members of the Matsui lab for their understanding, camaraderie, and willingness to help. I appreciate the friendships I have developed throughout the years. Growing up with Ross and Ted has been an amazing experience. I also can't thank them enough for sacrificing their sleep or weekends, at a moment's notice. I also appreciate Asma's help and mentorship, and her patience with me. Lukasz, Christian, and Gabriel have been great role models, and I would like to thank them for their insight as well. I have rarely met someone as caring as Qiuju. She single-handedly keeps the whole lab going forward. My mentees Chris, Karly, and Maya have taught me a lot of lessons, too. I also have not forgotten the kindness of Eun Hee, and the friendship of Yiting.

I would also like to thank Dr. Rajini Rao for her advice and career insight. Colleen and Leslie, you have made me feel welcome and appreciated, and I consider

Baltimore a second home. You have been there for me countless times and I cannot express how grateful I am.

I would not have been able to push myself if it wasn't for the love of my life, Claudia. I am eternally grateful for her love and faith in me, and I can't wait to start the next step of our adventure together. Nothing that I do would be possible without her grace and kindness.

My mom and dad, Nelly and Ruslan, have been with me through graduate school since the very beginning. They have supported and understood me, and nudged me when I needed a push. I can never repay their dedication to me, but I hope I've made them proud with my work.

My brother and sister, Rado and Luisa, have been with me throughout my journey as well, and I hope they know how much I appreciate them. Having them so close is a blessing, and their help and support have kept me going on numerous occasions.

I also want to thank all my friends who believed in me and pushed me along the way. Andi, David, Sheena, Usman, Achal, Nisha, Ars, Naveen, Kassa, Maya, Nasko, Viktor, Mitko, Katie, Rumen, Lubcho, Alko, Pesho, Vanka, Vasko, Naso, Paco, Dancho, Marto, Moni, Joro, Pafka, Stoyanov, Nixun, Rumen, Tosho, Peshka, Dobri, Mariq, Milena, Neli, I appeciate your support as well.

Table of Contents

List of tables

Tables

List of figures

Figures

Chapter 1

Identification of pancreatic cancer stem cells

Introduction

Pancreatic ductal adenocarcinoma (PDAC) carries one of the worst prognoses of any malignancy and is the fourth leading cause of cancer related deaths in the United States (1). Despite advances in better understanding the basic biology of PDAC, survival rates have not significantly improved over the past 30 years, and less than five percent of patients remain alive 5-years after diagnosis. Therefore, new treatments are needed for PDAC, and cancer stem cells (CSCs) have emerged as potential targets.

CSCs represent phenotypically distinct cells that possess enhanced tumor-initiating potential, self-renewal, and the ability to recapitulate the cellular heterogeneity of the original tumor (2). Since these initial findings, additional features including their rarity, relative chemoresistance, and metastatic potential have been described, and these properties have allowed them to be referred to by more precise terms, such as tumor initiating cells. However, due to the heterogeneous properties exhibited by CSCs, it has been difficult to provide a label capable of encompassing all of these attributes. Therefore, we will refer to these specialized cell populations by the general term CSC throughout this review. Although the identification of CSCs was limited to myeloid leukemias in the 1990s (3, 4), they have been described in an increasing number of solid tumors over the last decade, including multiple reports in PDAC (5-9). Several aspects of the CSC hypothesis have been hotly debated (10-12), but most relevant is their clinical significance. In PDAC, early data have suggested that the identification of CSCs in primary tumors is associated with shorter overall survival (6), and it is likely that additional functional properties including relative resistance to the standard cytotoxic

agent gemcitabine and enhanced metastatic potential are in part responsible for these findings (7, 13).

The identification and characterization of CSCs has generated novel hypotheses regarding the mechanisms involved in PDAC growth and dissemination, but several critical questions remain. We will initially review studies identifying pancreatic CSCs and speculate how these distinct cell populations may be related to one another. We will then discuss potential strategies to target pancreatic CSCs (14).

Identification of Pancreatic CSCs

At the most basic level, the CSC hypothesis links phenotypically defined tumor cells with specific functional properties, and CSCs have been stringently defined by their ability to differentiate and self-renew (15). The differentiation of CSCs gives rise to the full range of malignant cell types and histological recapitulation of the original tumor whereas self-renewal is responsible for maintaining long-term growth potential. In most diseases, the ability of putative CSCs to form tumors has been evaluated using immunodeficient mice (e.g., NOD/Scid and NSG) followed by histological examination and serial transplantation to demonstrate self-renewal (16). Although these mouse models remain the gold standard to evaluate CSCs, *in vitro* assays have also been developed to assess the clonogenic potential of CSCs including colony formation in semi-solid media or tumor sphere formation in liquid culture. Moreover, these *in vitro* assays may quantify the number of cells with self-renewal and long-term growth potential through serial rounds of plating.

Candidate CSC markers have largely consisted of differentially expressed cell surface antigens or drug resistance pathways. One approach to identify novel CSC populations has been the use of surface antigens expressed by normal stem cells in the tissue of origin, such as CD34 in myeloid leukemias (3, 17). Alternatively, antigens or enzymes capable of identifying normal stem cells in multiple tissues, such as CD133 and Aldehyde dehydrogenase (ALDH), have also been used to isolate CSCs in several diseases (18-22). Additionally, specific antigens associated with poor prognosis, such as CD44 or c-Met, have also served as CSC markers (5, 23-25). Finally, recent work makes

use of distinct metabolic features of CSCs, such as riboflavin accumulation, in order to isolate them (8).

The initial identification of pancreatic CSCs extended ground-breaking work in breast cancer and investigated the expression of CD44, CD24, and epithelial specific antigen (ESA) (Table 1) (5, 14). Relative to unsorted cells, $CD44^{+}CD24^{+}ESA^{+}$ cells isolated from low-passage PDAC xenografts were highly tumorigenic and recapitulated the histology and cellular heterogeneity of the original tumor. Furthermore, the functional differences between $CD44^{+}CD24^{+}ESA^{+}$ and $CD44^{-}CD24^{-}ESA^{-}$ cells were maintained following subcutaneous or orthotopic injection suggesting that tumorigenic potential was cell autonomous and independent of local environmental factors. A second report demonstrated that CD133 could also identify pancreatic CSCs (7). In addition to being highly tumorigenic, $CD133^{+}$ pancreatic cancer cells were found to be relatively resistant to gemcitabine treatment compared to $CD133^{-}$ cells.

Cellular markers associated with drug resistance have also been used to identify CSCs. ALDH, specifically ALDH1A1, is required for the synthesis of all-*trans*-retinoic and high enzyme activity marks normal mouse pancreatic progenitor cells and normal human stem cells in several organ systems (26, 27). ALDH may also play a role in drug resistance as it can metabolize and neutralize specific cytotoxic alkylators, such as cyclophosphamide. We studied ALDH in PDAC and found that $ALDH^{+}$ cells are highly tumorigenic compared to bulk tumor cells (6, 28). Moreover, $ALDH^{+}$ cells appear to be relatively resistant to gemcitabine *in vivo* and have increased invasive potential suggesting a role in disease progression (6, 13).

Despite the importance of CD44, CD133, and ALDH in identifying pancreatic CSCs, it is unclear whether these antigens are involved in regulating CSC function or merely serve as phenotypic markers. However, other pancreatic CSC markers have been identified that may be functionally relevant. For example, CXCR4 serves as the chemokine receptor for Stromal cell-derived factor-1 (SDF-1, CXCL12) and is expressed by a subset of $CD133^+$ CSCs that have enhanced metastatic capacity (7). Recent studies have also demonstrated that c-Met can identify and regulate pancreatic CSCs similar to findings in glioblastoma (25, 29). Thus, several strategies have been used to identify pancreatic CSCs, and some of these may provide insights into regulatory factors and potential targeting strategies.

Figures and tables

Table 1(14). Phenotype and functional properties of pancreatic CSC populations.

Study	Phenotype	Properties
Li *et al*.(30)	$CD44^+CD24^+ESA^+$	Increased Sonic Hedgehog expression.
Hermann *et al*.(7)	$CD133^+$	Chemoresistant. $CD133^+CXCR4^+$ cells responsible for metastasis.
Rasheed *et al*.(31) Ishizawa *et al*.(28)	$ALDH^+$	CSCs associated with overall survival. CSCs exhibit mesenchymal feature and are frequently found in metastatic lesions. $ALDH^+$ and $CD44^+CD24^+$ cells are equally tumorigenic.
Li *et al*.(25)	$CD44^+$c-Met^+	Highly metastatic.
Miranda-Lorenzo *et al.(8)*	Autofluorescent	Chemoresistant Highly metastatic

Chapter 2

The relationship between distinct cancer stem cell populations

Introduction

In most normal organ systems, such as the blood, CNS, and skin, cells are functionally and phenotypically organized according to a strict cellular hierarchy in which self-renewing stem cells give rise to short lived progenitors then terminally differentiated effector cells. The earliest studies in acute myeloid leukemia (AML) demonstrated that tumor cells resembling normal hematopoietic stem cells can self-renew and give rise to relatively differentiated and non-tumorigenic blasts (4). Therefore, it has been generally assumed that cancers are organized in a hierarchical manner similar to normal tissues. However, several CSC populations have been identified in PDAC, and it is not clear how each of these fits into a specific hierarchy or are related to one another. One possibility is that all of the current markers recognize the same cell, but the vast majority of $ALDH^+$ pancreatic tumor cells appear to lack CD44 and CD133. Therefore, it is likely that these antigens identify at least two, or even three, unique cell populations (6, 32). Alternatively, since each putative CSC marker enriches for cells with increased tumorigenic potential but fails to isolate pure populations of CSCs (*i.e.*, every cell expressing a specific marker is not tumorigenic), it is possible that combining antigens will greatly increase CSC purity. However, this does not appear to be the case as the tumor initiating cell frequency of rare PDAC cells co-expressing CD44, CD24, and ALDH is not significantly greater than either $ALDH^+$ or $CD44^+CD24^+$ cells (28). Moreover, c-Met is expressed, albeit at variable levels, on $CD44^+$, $CD133^+$, or $ALDH^+$ cells, but increased tumorigenic potential is limited to $CD44^+$c-Met^{high} cells (25). Delineating the relationship between these populations is a critical step in the

development of successful therapies since all self-renewing cells within a pancreatic tumor must be targeted and eliminated. Therefore, we tested whether pancreatic adenocarcinoma cells are organized as a hierarchical system with a phenotypically defined stem cell at the apex.

Methods

Cell culture

Capan-1 cells were obtained from the American Type Culture Collection (Manassas, VA) global bio-resource center and authenticated by short tandem repeat profiling at the Johns Hopkins Genetics Core Resources Facility. Cells were cultured in high glucose Dulbecco's modified Eagle medium (Invitrogen, Carlsbad, CA) supplemented with 10% fetal bovine serum (Sigma-Aldrich, St. Louis, MO), 1% penicillin-streptomycin (Invitrogen), and1% L-glutamine (Invitrogen). Cells were cultured in normal 35-mm culture dishes (Corning, Corning, NY), and normal 25cm^2, and 75cm^2 tissue culture flasks (Sarstedt, Nümbrecht, Germany).

Animal care and patient derived xenografts

All experiments using mice were approved by the Johns Hopkins University Animal Care and Use Committee and the mice were maintained in accordance with the American Association of Laboratory Animal Care guidelines. Low passage xenografts were generated of surgical specimens derived from patients undergoing surgery at the Johns Hopkins Hospital. Freshly collected tumors were implanted subcutaneously into 6-week-old female athymic nude mice (Harlan), and following growth to 1.5 cm^3 they were excised and transplanted to secondary recipients.

To generate cell line and patient xenogratfts we resuspended cells in serum-free DMEM and Matrigel (BD Biosciences, San Jose, CA) in a 1:1 ratio and then injected them (in 100 µL volume) subcutaneously into the flanks of NOD/SCID mice lacking the interleukin-2 receptor gamma chain (NSG).

Flow cytometry and cell sorting

Single cell suspensions from cell line-derived and patient-derived xenografts were prepared by mincing tumors using sterile razor blades, followed by mechanical and enzymatic dissociation using the MACS Dissociation Kit (Miltenyi Biotec, San Diego, CA) (cite). Tumor debris and necrotic cells were depleted using a 70-μm filter (BD Biosciences) and density centrifugation using Ficoll-Paque Plus (GE Healthcare, Marlborough, MA).

Cells were then stained with the ALDEFLUOR reagent (Stem Cell Technologies, Vancouver, Canada) for 30 minutes in a 37°C water bath according to the manufacturer's protocol. Next they were stained for 15 min at 4°C with anti-mouse CD31-biotin (BD Biosciences), anti-mouse lineage-biotin (Miltenyi Biotec), and anti-mouse H-2K^{d}-biotin (BD Biosciences) antibodies. They were then washed, and stained for 15 min at 4°C with Streptavidin–PerCP (BD Biosciences), followed by a wash and a staining at 4°C for 20 min with anti-CD44-APC (clone G44-26, BD Biosciences) and anti-CD24-PE (clone ML5, BD Biosciences). A FACSAria II Flow Cytometer (BD Biosciences) and BD Facscalubur (BD Biosciences) were used for cell sorting and analysis respectively.

Results

Tumors derived from distinct CSCs, and non-CSCs exhibit identical phenotypic composition

In order to study the relationship of distinct CSC populations, we injected Capan-1 cells subcutaneously into the flanks of NSG mice and allowed tumors to develop for three weeks. These tumors were then collected, sorted into non-overlapping $CD24^+CD44^+$ and $ALDH^+$ cells, and cells that did not express any of these markers, and injected into the flanks of NSG (Fig 1). After six weeks the resulting tumors were examined for the presence of different phenotypic populations by flow cytometry. Interestingly, the cellular diversity characteristic of the original tumors was present in the tumors derived from each sub-population (Fig 2a). We also studied patient derived pancreatic cancer tumors continuously passaged in immune deficient mice (xenografts) that have been extensively studied by full exomic sequencing and gene expression profiling[6]. We used these tumors in order to capture the biology of pancreatic cancer that occurs in the clinical setting and more precisely examine the relationship between distinct cancer stem cell populations. We grew Panc219 tumors subcutaneously in NSG mice and isolated $CD24^+CD44^+$ and $ALDH^+$ cells, and cells that did not express any of these markers. Eight weeks after we injected the sorted cells we looked for the presence of different populations by flow cytometry. Regardless of their origin, the tumors exhibited striking similarity (Fig 2b). Thus multiple non-overlapping cell populations can recapitulate the original tumor heterogeneity.

Discussion

We have demonstrated that two distinct largely non-overlapping CSC populations ($CD24^+CD44^+$ and $ALDH^+$ cells) derived from pancreatic both cancer cell lines and patient derived sample can recapitulate the original phenotypic diversity in an *in vivo* setting. Importantly cells that did not express these CSC markers were able to do so, as well. Our results demonstrate that $CD24^+CD44^+$ and $ALDH^+$populations might not display a hierarchical relationship but can give rise to one another. Interestingly our data suggests that cells lacking these markers could also generate cancer stem cells. Therefore, we now believe that the cellular organization of pancreatic cancers could be characterized by a high degree of plasticity.

The significance of the various pancreatic CSC markers and the cells they identify clearly requires further clarification (14). If multiple CSC populations actually exist, an understanding of how they are related to one another will be important since clinically effective targeting likely requires the elimination of all self-renewing cells within the tumor. It is still PDAC cells are organized in a hierarchical and linear manner with a single, phenotypically distinct, still unidentified, CSC, at the apex giving rise to the other CSC populations and ultimately non-clonogenic mature tumor cells (Figure 3) (14). It is also possible that each phenotypically distinct CSC population represents a specific cellular state of the same clonogenic cell that gives rise to mature tumor cells. Another possibility is that each CSC population is unrelated to another and parallel lines of mature tumor cell production exist. Finally, it is conceivable that a rigid hierarchy of unidirectional differentiation does not exist, but that the system is plastic with non-

clonogenic cells giving rise to tumorigenic CSCs displaying a variety of phenotypes.

Beyond the organization of phenotypically defined CSC populations, it is also unclear whether the various CSCs are functionally similar or distinct. Although tumor formation, histologic recapitulation, and self-renewal define CSCs, other properties, including relative drug resistance, invasion, migration, and metastatic potential have been ascribed to CSCs and may contribute to their clinical impact (33). It is possible that certain CSC populations could be primarily responsible for tumor initiation and maintenance at the primary site of disease, whereas others could be responsible for tumor dissemination and growth at metastatic sites, such as the subpopulation of $CD133^+$ CSCs expressing CXCR4 (7). It is also possible different organs, such as the liver and lung, harbor different microenvironments with distinct endothelial or stromal cell types or extracellular matrix components that promote or inhibit tumor growth (Figure 4) (34). Therefore, if metastatic dissemination depends on the interaction of CSCs with a particular niche, then different niches might call for unique CSCs. An evaluation of the tumor forming potential of specific CSCs at orthotropic and different metastatic sites may determine whether certain populations are better suited to grow within particular locations.

It is also possible that the phenotypes exhibited by CSCs are dictated by the external microenvironment. For example, pancreatic tumors are characterized by desmoplasia and dense fibrosis that may expose cells to relative hypoxia, and the hypoxic state has been found to alter the expression of the CSC marker CD133 in brain tumors (35). In addition, several markers used to identify CSCs, such as ALDH and the side population assay, are indicative of drug resistance mechanisms and it is possible that their

expression is induced in response to cellular damage. Finally, it is possible that the adaptive metabolic changes undertaken by tumor cells also modifies the expression of CSC makers, although such findings have yet to be reported (36).

Studies have demonstrated a clear link between CSCs and the epithelial-to-mesenchymal transition (EMT) in solid tumors. Therefore, it is possible that CSCs represent a specific cellular state expressing multiple phenotypes. Reports using breast cancer models have demonstrated that the induction of EMT by TGF-β or the modulation of specific gene expression (*e.g.*, induction of *Twist* or repression of *E-Cadherin*) results in increased expression of CD44 and tumorigenic potential (37, 38). In pancreatic cancer, $ALDH^+$ cells appear have a gene expression profile consistent with EMT and increased invasive and migratory potential compared to bulk tumor cells and $CD44^+CD24^+$ cells (6). Moreover, studies examining ZEB1, an inducer of EMT, in pancreatic cancer cells have identified a direct link between EMT, increased tumorigenicity, and drug resistance (39). Therefore, it is possible that a more "epithelial" or "mesenchymal" state is important in determining the functional properties of CSCs. The specific functional properties of different pancreatic CSCs are unclear, and the quantification of tumor formation, metastatic potential, and drug resistance is needed.

Inter-patient heterogeneity may also contribute to the existence of multiple pancreatic CSCs. Recurrent genetic alterations are a hallmark of cancer, and mutations in *KRas* are present in the vast majority of PDAC (40, 41). On the other hand, mutations in other genes, such as *p53* and *Smad4/DPC4*, can be identified in some, but not all tumors (42, 43). Therefore, pancreatic cancers are not genetically homogeneous, but vary from patient to patient (44). If alterations in specific genes are prognostic and CSCs truly

dictate the natural history of PDAC given their potential roles in tumor formation, drug resistance, and metastatic progression, it is likely that specific mutations influence both the phenotype and function of CSCs. Currently, it is unclear whether phenotypically identical CSCs from different patients have the same functional attributes and contribute to disease progression in similar ways. However, such a finding would imply that personalized and individualized CSC targeting therapies are needed. In order to examine inter-patient diversity, the functional properties of different CSCs derived from human tumors with distinct genotypes will need to be determined. In addition, the examination of CSC phenotypes and functional properties in tumors derived from transgenic animal models of pancreatic cancer may be particularly helpful since specific genetic lesions can be modulated in these systems (45).

To further complicate matters, increasing evidence suggest that human cancers can be genetically heterogeneous within the same individual (46-49). Therefore, intra-patient genetic heterogeneity may also drive the phenotypic and functional diversification CSCs. In many cancers, including PDAC, specific genetic alternations may accumulate in an orderly fashion during disease progression (50, 51), Thus, it is also possible that different CSCs are responsible for relapse and progression over the course of the disease. In PDAC, metastatic lesions may be genetically distinct from one another and the primary tumor (52). Moreover, primary tumors are composed of geographically and genetically distinct subclones. The role of genetic evolution and diversification in the emergence of distinct CSCs, or conversely, the impact of CSCs on the clonal composition of an individual tumor is not entirely clear, but it is likely that these two processes interact at some level. Therefore, pancreatic CSCs may be phenotypically and

functionally distinct at specific anatomical sites or at each stage of clinical disease. A systematic investigation of genetic lesions within CSCs, their phenotypes, and functional properties, such as tumorigenic potential, metastasis, and drug resistance, within primary tumors and metastatic lesions derived from the same patient may address this possibility.

Figure Legends

Figure 1. Experimental design. Human xenografts were sorted based on cell surface expression of CD24 and CD44, and activity of Aldehyde dehydrogenase (ALDH). Secondary xenografts were generated from the sorted populations and their phenotypic diversity was examined by flow cytometry.

Figure 2. Phenotypic plasticity between CSCs and non-CSCs. Tumors derived from sorted Capan-1 (A) or Panc 253 (B) xenografts exhibit identical phenotypic composition regardless of the cell of origin.

Figure 3. Potential relationships between CSCs and mature tumor cells. (A) A linear organization with a single phenotypically distinct CSC giving rise to the other CSC populations and ultimately non-clonogenic mature cells. (B) Each phenotypic CSC represents a distinct state of the same clonogenic cell that gives rise to the mature tumor cell. (C) Each CSC population is unrelated to another and parallel lines of mature tumor cell production exist. (D) A plastic system in which non-clonogenic mature cells give rise to CSC displaying a variety of phenotypes.

Figure 4. Potential functional relationships between CSCs. (A) Distinct CSCs may give rise to macroscopic tumors in distinct anatomical locations. Each population is responsible for tumor growth and resistance to therapy in different organs. (B) A primary CSC population is responsible for tumor initiation and growth at the primary site.

Additional populations are responsible for initiation and maintenance at metastatic sites and for resistance to chemotherapy.

Figures and tables

Figure 1

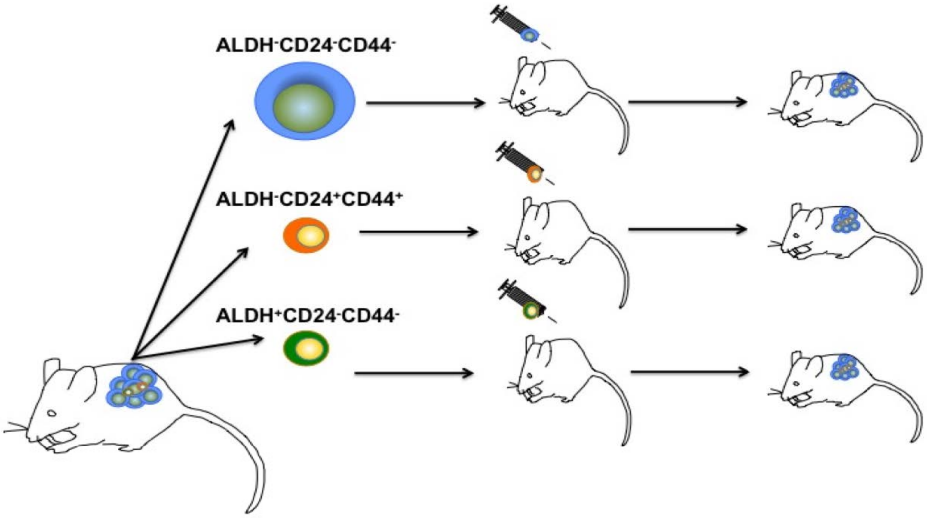

Figure 2

A

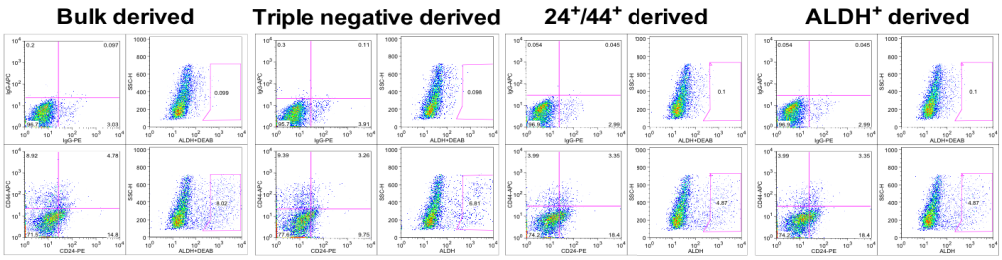

B

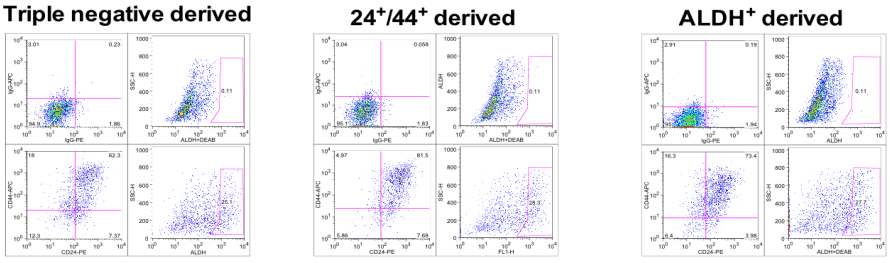

Figure 3

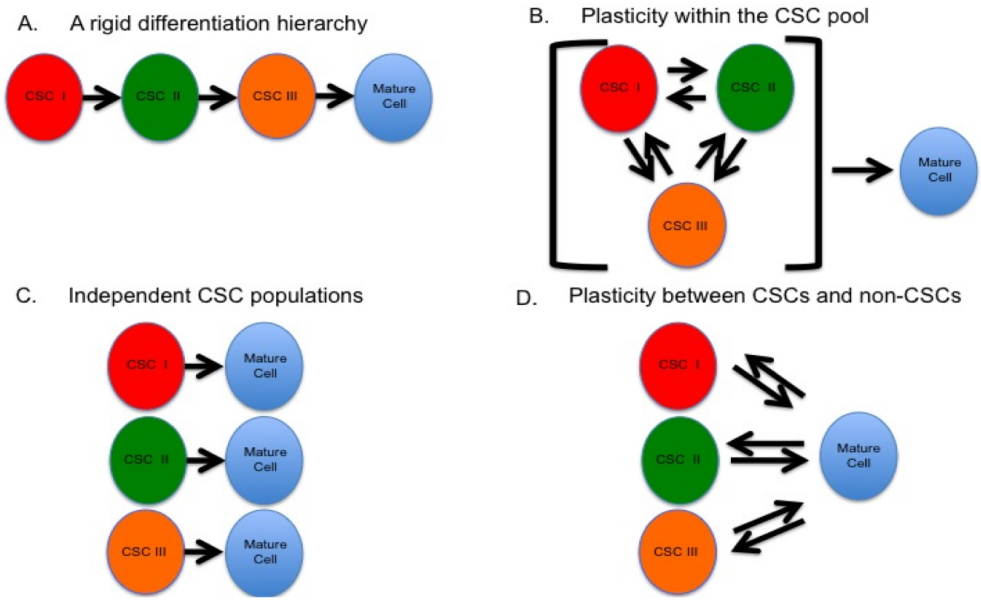

Figure 4

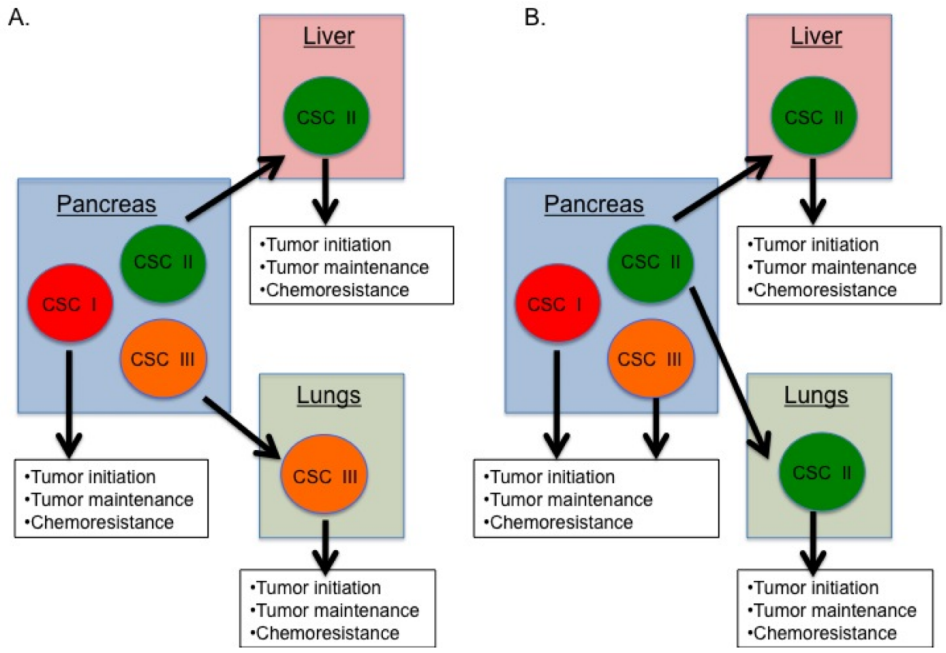

Chapter 3

Regulation of cancer stem cell functions by actin filament dynamics

Introduction

The self-renewal potential and resistance to traditional cytotoxic agents suggest that successful CSC targeting strategies will improve clinical outcomes. One potential approach is targeting the cell surface antigens that characterize pancreatic CSCs using monoclonal antibodies. For example, a bi-specific antibody recognizing both ESA and CD3 has been found to eliminate pancreatic CSCs by redirecting cytotoxic T-lymphocytes (53). CD44 is another surface protein expressed by CSCs in multiple diseases (54), and a specific monoclonal antibody against CD44 can eliminate AML stem cells by inducing terminal differentiation (55). The functional activities of specific pancreatic CSC markers may also serve as potential targets (Table 1). The hepatocyte growth factor (HGF) receptor c-Met identifies highly tumorigenic CSCs in combination with CD44, and the pharmacological inhibition of its activity has been found to inhibit tumor growth and metastasis (25). CD47 is expressed preferentially on $CD133^+$ cells and normally protects them from being phagocytosed by macrophages (56). Inhibition of CD47 enhances phagocytosis of CSCs and also directly induces their apoptosis. Another functionally relevant marker is CXCR4 that plays an important role in the homing of hematopoietic stem cells to the bone marrow. CXCR4 has been identified on a subset of $CD133^+$ pancreatic CSCs with enhanced metastatic capacity, and CXCR4 antagonists may prevent tumor dissemination (7). Another potential cell surface target is Death receptor 5 (DR5) that induces apoptosis following binding to TRAIL. A recent study found that $ALDH^+$ and $CD44^+CD24^+$ pancreatic CSCs express relatively increased levels of DR5, and receptor engagement using an agonistic monoclonal antibody markedly reduced CSC frequency and tumor growth *in vivo* (57).

Several cellular signaling pathways have been identified that regulate the self-renewal of normal stem cells and may serve as targets against CSCs. These include pathways required for normal embryonic development, and the Hedgehog (Hh), Notch, and Nodal/Activin pathways may be active in pancreatic CSCs. Nodal and Activin are ligands of the TGF-β superfamily, and a recent study demonstrated that these ligands and their receptor ALK4 are overexpressed in pancreatic CSCs (58). The pharmacological inhibition or knockdown of ALK4 abrogated self-renewal and tumorigenicity as well as sensitized CSCs to gemcitabine. Another series of studies has examined the Hh signaling pathway in pancreatic CSCs and found that-pharmacological pathway inhibition reduced the frequency of CSCs and decreased tumor formation and metastasis (13, 59, 60). Of note, a recent phase 2 clinical trial compared gemcitabine alone or in combination with the novel Hh inhibitor saridegib (IPI-926) in patients with metastatic pancreatic cancer based on preclinical data demonstrating enhanced responses to cytotoxic chemotherapy (61). A higher rate of progressive disease was observed at an interim analysis in patients receiving saridegib (http://phx.corporate-ir.net/phoenix.zhtml?c=121941&p=irol-newsArticle&ID=1653550&highlight=). Although the precise reasons for these results are unclear, it is possible that the Hh pathway regulates the development, rather than maintenance, of metastatic lesions and other ongoing trials of Hh inhibitors in the neoadjuvant setting may provide a better scenario to detect these potential anti-CSC effects. Finally, the inhibition of Notch signaling has been found to inhibit EMT and cellular invasion as well as decrease the frequency of $ALDH^+$ CSCs (62). Thus, cellular pathways involved in regulating the self-renewal of normal stem cells may represent pancreatic CSC targets.

Differential metabolic requirements of CSCs can also serve as a method for targeting them. PDAC CSCs are dependent on oxdative phosphorylation (OXPHOS), and can have very limited metabolic plasticity(63). The anti-diabetic drug metformin decreases tumor growth and initiation. Combining metformin with the bromodomain family of proteins inhibitor JQ1 targets CSCs and prevents the emergence of metformin resistant clones.

The association of EMT and CSCs may also form the basis for identifying novel targeting agents. High-throughput strategies to screen for novel anti-CSC compounds have been difficult to carry out because of the lack of pure CSC populations and the complex nature of the assays used to assess their functions, but several methods may induce EMT and increase the frequency of CSCs. This approach was ingeniously used by Gupta *et al*. who genetically engineered human breast cancer cell lines to induce EMT and screened for compounds that could induce cell death (37). The ionophore salinomycin was identified as a potential CSC targeting agent then subsequently found to block tumor formation and metastasis *in vivo*. Shortly thereafter, salinomycin was shown to inhibit the growth of pancreatic CSCs, indicating that it may represent a potential CSC targeting agent in multiple malignancies (64). Therefore, similar strategies based on EMT may identify novel agents that inhibit pancreatic CSCs.

Strategies eliminating one or two specific CSC populations might have a limited success since a successful treatment would need to eradicate all sources of self-renewal within the tumor. It is critical to determine whether there are fundamental processes that regulate CSC functions, regardless of the underlying phenotype. Targeting multiple populations is more likely to improve disease outcome.

An area of investigation that has gained increased interest over the past ten years is the regulation of cell fate commitment by actin dynamics. In several contexts changes in cell shape dictate differentiation decisions (65-71). The driver of these cell shape induced decisions is a shift in actin polymerization dynamics. Keratinocyte differentiation is regulated by the balance between polymerized (F-actin) and free actin (G-actin), where a lower F/G actin ratio drives stem cell maintenance (65). In embryonic stem cells (ESCs) a blockade of actin polymerization leads to the maintenance of self-renewal and negates the need of Leukemia Inhibiting Factor (LIF) to maintain the cells in an undifferentiated state (67). In the case of mesenchymal stem cells (MSCs), actin dynamics determine osteogenic versus adipogenic differentiation (69). Furthermore, changes in actin polymerization and organization in MSCs can override soluble differentiation signals (69). Given that regulation of differentiation by modulation of actin dynamics is a mechanism present in multiple systems we hypothesized that it is also active in the maintenance of CSCs.

When we were devising a strategy to study the biology of actin polymerization and organization in CSCs we wanted to find a reliable method to examine these characteristics. Additionally, it was our desire to find a way to target the processes pharmacologically in order to explore potential therapeutic strategies. We decided to investigate actin dynamics in CSCs by modulating the expression and activation of the membrane-actin linker protein Ezrin.

Ezrin is a member of the Ezrin-Radixin-Moesin (ERM) family of proteins that function by connecting molecules on the plasma membrane to the actin cytoskeleton (72-74). Ezrin is kept inactive in the cytoplasm by a head-to-tail interaction between its N-

terminus and C-terminus. Upon activation and interaction with PIP_2, Ezrin assumes an unfolded conformation that allows phosphorylation of a threonine residue at position 567 in its C-terminus. This phosphorylation is necessary for Ezrin to bind to actin filaments with its C-terminal domain. With its N-terminal FERM domain the protein binds cell surface receptors or channels through their cytoplasmic tails or through adaptor proteins.

Modulation of Ezrin expression or activity alters cell shape and actin filament organization in multiple systems (75-79). Additionally, Ezrin can be found in a complex with two of the cell surface markers used to identify PDAC CSCs as its N-terminal domain Ezrin binds to the cytoplasmic tail of CD44 (80). Ezrin is also a substrate for the receptor tyrosine kinase HGF/c-Met and its association with CD44 is necessary for c-Met-mediated signal transduction (81-83). Thus Ezrin suggested a potential link between CSC associated surface antigens and cytoskeletal dynamics.

Recently, we have identified a pharmacological agent (Drug 8) that inhibits Ezrin-actin interaction (84). Additionally, the levels of Ezrin expression or activation are a predictor of decreased survival or the development of distant metastases in multiple cancers, indicating its importance in tumor biology (85-92). In PDAC the expression levels of Ezrin itself do not correlate with negative outcomes, however, phosphorylation of Ezrin, associated with growth factor receptor activation predicts shorter overall survival (93-95). Experiments in PDAC cell lines indicate that Ezrin mediates growth and motility, but its role in cytoskeletal remodeling and CSC biology has not been investigated (96, 97). Thus we chose Ezrin as both a tool to study the role of actin dynamics in CSC biology and a potential therapeutic target.

Our studies identified modulation of actin dynamics as a novel mechanism of regulation of CSC functions. In PDAC, Ezrin maintains a CSC-associated actin state, at least in part, by antagonizing ROCK signaling.

Methods

Cell culture

L3.6pl, E3LZ 10.7, and MIA PaCa-2 cells were obtained from the American Type Culture Collection (Manassas, VA) global bio-resource center and authenticated by short tandem repeat profiling at the Johns Hopkins Genetics Core Resources Facility. All cell lines were cultured in high glucose Dulbecco's modified Eagle medium (Invitrogen, Carlsbad, CA) supplemented with 10% fetal bovine serum (Sigma-Aldrich, St. Louis, MO), 1% penicillin-streptomycin (Invitrogen), and1% L-glutamine (Invitrogen). Cells were cultured in normal 35-mm culture dishes (Corning, Corning, NY), and 25cm^2, and 75cm^2 normal tissue culture flasks (Sarstedt, Nümbrecht, Germany)

An siRNA sequence against Ezrin was obtained from GE Dharmacon (Lafayette, CO; siRNA1 cat. #: NM001111077). A short hairpin RNA (shRNA) oligonucleotide was generated from this sequence and cloned into the Tet-pLKO-puro lentiviral vector (Addgene, Cambridge, MA). An shRNA sequence against the Luciferase gene was used as a control construct. Cell lines were transduced and stable lines were selected using puromycin (Thermo Fisher Scientific, Waltham, MA).

A complementary DNA (cDNA) sequence of Ezrin, containing a threonine to aspartic acid substitution at residue 567 was obtained from Aykut Uren's laboratory at Georgetown University (Washington, DC). The cDNA was cloned into the pInucer20 lentiviral vector using the Gateway cloning system (Thermo Fisher Scientific) (98). A self-ligated empty pInducer20 construct was used as a control. Cell lines were transduced and stable lines were selected using G418 sulfate (Corning).

Animal care, low passage derived patient xenografts, and tumorspheres

All experiments using mice were approved by the Johns Hopkins University Animal Care and Use Committee and the mice were maintained in accordance with the American Association of Laboratory Animal Care guidelines. Low passage xenografts were generated of surgical specimens derived from patients undergoing surgery at the Johns Hopkins Hospital. Freshly collected tumors were implanted subcutaneously into 6-week-old female athymic nude mice (Harlan), and following growth to 1.5 cm^3 they were excised and transplanted to secondary recipients.

Single cell suspensions from patient-derived xenografts were prepared by mincing tumors using sterile razor blades, followed by mechanical and enzymatic dissociation using the MACS Dissociation Kit (Miltenyi Biotec, San Diego, CA) (31). Tumor debris and necrotic cells were depleted using a 70-μm filter (BD Biosciences) and density centrifugation using Ficoll-Paque Plus (GE Healthcare, Marlborough, MA). Cells were then labeled using anti-mouse CD31-biotin (BD Biosciences), anti-mouse lineage-biotin (Miltenyi Biotec), and anti-mouse H-2Kd-biotin (BD Biosciences) antibodies, followed by incubation with ant-biotin-coupled magnetic microbeads (Miltenyi Biotec). Mouse-derived cells were depleted using a MACS Cell Separation LD Column (Miltenyi Biotec). Cells were washed twice in cold phosphate buffer saline (PBS) (Invitrogen) and manually counted using a hemocytometer.

For generation of tumorspheres, 200,000 cells/ml were plated in DMEM/F-12 (1/1) media (Invitrogen) supplemented with 1X B-27 supplement (Thermo Fisher Scientific), 20ng/ml bFGF (Invitrogen), 1% penicillin-streptomycin (Invitrogen), and 1% L-glutamine (Invitrogen). Cells were cultured in 60-mm ultralow attachment tissue

culture dishes (Corning). After 7-10 days spheres were selected by washing trough a 40-μm Filter (BD Biosciences). They were then dissociated enzymatically with 0.05% Trypsin (Invitrogen) and plated at $2*10^3$ cells/ml for differentiation studies or $1*10^4$ cells/ml for Drug8 treatments or maintenance of spheres.

In vivo limiting dilution assay

To measure tumor-initiating cell frequency (TIF), we resuspended 100,000 L3.6pl cells containing the Tet-pLKO-puro construct in serum-free DMEM and Matrigel (BD Biosciences) in a 1:1 ratio and then injected them (in 100-μL volume) subcutaneously into the flanks of NOD/SCID mice lacking the interleukin-2 receptor gamma chain (NSG). The tumors were allowed to grow until a volume of approximately $100mm^3$ after which their drinking water was substituted for 2mg/ml of Doxycycline (Sigma-Aldrich) in 5% sucrose solution (Sigma-Aldrich). Control mice from both groups received only a 5% Sucrose solution (Sigma-Aldrich). Tumors were measured after 3, 6, and 9 days in 2 perpendicular dimensions and tumor volume was calculated using the formula for prolate ellipsoid: $mm^3 = (L \times W^2)/2$. After 9 days of treatment the tumors were collected, dissociated, and depleted from mouse cells according to protocol. They were washed in cold serum-free DMEM twice, and manually counted using a hemacytometer. Next they were resuspended in serum-free DMEM and Matrigel (BD Biosciences) in a 1:1 ratio and then injected (in 100μl volume) subcutaneously in the flanks of NSG mice in limiting dilutions (500, 250, 100, 50 cells). Mice were monitored for tumor formation for 30 days. Tumor initiation frequency was calculated using extreme limiting dilution analysis (ELDA) (99).

Flow cytometry

Cells from patient derived xenografts were stained for 15 min at 4°C with anti-mouse CD31-biotin (BD Biosciences), anti-mouse lineage-biotin (Miltenyi Biotec), and anti-mouse H-2K^{d}-biotin (BD Biosciences) antibodies. They were then washed, and stained for 15 min at 4°C with Streptavidin–PerCP (BD Biosciences), followed by a wash and a staining at 4°C for 20 min with anti-CD44-APC (clone G44-26, BD Biosciences), anti-CD24-PE/FITC (clone ML5, BD Biosciences), anti-c-Met-PE (clone 95106, R&D Systems, Minneapolis, MN), and anti CD133-APC (Clone AC133, Milteniy Biotec).

For intracellular staining, cells were fixed and permeabilized for 30 min at 4°C with Cytofix/Cytoperm buffer (BD Biosciences). They were washed and incubated in 5% Bovine Serum Albumin (BSA) and 2mM EDTA in PBS for 1hr at room temperature. Then they were washed and stained for 1 hour at room temperature in the dark with rabbit polyclonal anti-Ezrin (Cell signaling, Danvers, MA, 1:50 dilution), rabbit polyclonal anti-pERM (Cell signaling, 1:1000 dilution), phalloidin-TRITC/FITC (Sigma-Aldrich, 125 ng/ml), and DNAse1-AlexaFluor488 (Sigma-Aldrich, 500 ng/ml) in 0.5% BSA and 2mM EDTA in PBS. Cells were washed and then incubated with goat anti-rabbit-AlexaFluor488 (Invitrogen, 1:1000 dilution) for 1 hr at room temperature in the dark. They were then washed and a BD FACScalibur (BD Biosciences) was used for analysis.

Cells from cell lines and tumorspheres were not labeled with with anti-mouse CD31-biotin (BD Biosciences), anti-mouse lineage-biotin (Miltenyi Biotec), and anti-mouse H-2K^{d}-biotin (BD Biosciences) antibodies. They were stained with the rest of the antibodies according to protocol.

Quantitative real-time PCR analysis

Total mRNA was extracted using and depleted of genomic DNA using the RNeasy PlusMini Kit (Qiagen, Germantown, MD). It was reverse-transcribed with SuperScript III reverse transcriptase (Invitrogen). qRT-PCR was performed using Taqman Probes (GAPDH probe #: hs099999905, Ezrin probe #:hs00931653) (Applied Biosystems, Foster City, CA).

Colony formation assay

One thousand cells were suspended in 1ml of 1.2% methylcellulose (Sigma-Aldrich), 30% fetal bovine serum (Sigma-Aldrich), 1 %BSA (Sigma-Aldrich), 1% penicillin-streptomycin (Invitrogen), 1% L-Glutamine (Invitrogen), and 10^{-4}M 2-mercaptoethanol in RPMI medium (Invitrogen). Samples were plated in duplicate in 35-mm ultralow attachment tissue culture dishes (Corning) and incubated at 37^{o}C. Colonies were scored after 12-15 days. Serial replating was carried out by washing the plates 3 times with serum-free RPMI media, resuspending the cells in the original volume of methylcellulose, and re-plating according to protocol.

Migration assay

Six hundred thousand (L3.6pl) or 200,000 (E3LZ 10.7, MIA PaCa-2) cells suspended in DMEM supplemented with 1% FBS were applied to 24-well cell culture inserts with 8-μm pores (BD Biosciences). The cell culture inserts were immersed in DMEM supplemented with 10% FBS. The cells were cultured at 37^{o}C and 5% CO_2, and after 24 hours the cells remaining above the filter were removed. The filter membrane

was removed and fixed onto a frosted microscope slide (Thermo Fisher Scientific), using ProLong Gold Antifade Reagent with DAPI (Life Technologies), and coverslipped with a microscope cover grass (Thermo Fisher Scientific). After 24 hours pictures of the slides were taken with a Nikon Eclipse Ti fluorescent microscope (Nikon, Minato, Tokyo, Japan). The number of DAPI nuclei in three random fields from each slide was calculated using the NIS Elements software (Nikon).

Immune fluorescence

Cell lines were grown on on LAB-Tek II 4-well glass slides (Thermo Fisher Scientific). Prior to staining cells were washed with PBS three times and fixed with 4% Formalin for 15 min at room temperature, after which they were washed 10 times with PBS. After fixation they were incubated in 5% BSA and 0.3% Triton-X (Sigma-Aldrich) in PBS for 1 hour at room temperature. The buffer was aspirated and the cells were stained in 1%BSA and 0.3% in Triton-X PBS with Phalloidin-TRITC (Sigma-Aldrich, 125ng/ml) and DNAse1-Alexafluor488 (Sigma-Aldrich, 10ug/ml) for 1 hr at room temperature in the dark. Then cells were washed 10 times with PBS and coverslipped with a microscope cover grass (Termo Fisher Scientific) using Prolong Gold Antifade reagent with DAPI (Life Technologies). Pictures were taken with a Nikon Eclipse Ti fluorescent microscope (Nikon) using the NIS Elements software (Nikon).

Tumorspheres were collected and suspended in 250uL PBS then fixed on glass Shendon cytospin slides (Thermo Fisher Scientific) by centrufugation in a Cytospin4 centrifuge (Thermo Fisher Scientific) at 800rpm for 5 minutes. They were then air-dried for 3 minutes and processed as described above.

Drug treatments

Compound NSC305787 (Drug 8) was obtained from Aykut Uren's laboratory at Georgetown University (Washington, DC).

Cell lines were treated with 1uM of the drug for 72 hours in regular cell culture dishes after which they were collected by trypsinization and plated in a colony-forming assay in methylcellulose.

Tumorspheres were plated at a density of 10,000 cells/ml and after three days they were treated with 1uM of the compound. After an additional 72 hrs they were collected, enzymatically broken down to single cells and half of all remaining cells were suspended in 2ml media. The number of spheres formed after 7 days was scored.

Cytochalasin D (Tocris Biosciences, Bristol, United Kingdom) and Y-27632 dihidrochloride (Sigma-Aldrich) were resuspended according to manufacturer's protocol. Cell lines were treated with the compounds in regular cell culture dishes after which they were collected and plated as single cells in colony forming assay in methylcellulose.

Statistics

Statistical differences between two normalized groups were analyzed using a one-sample t-test (GraphPad Prism Software, Inc). Statistical differences between non-normalized groups were analyzed using the two-tailed unpaired Student t-test (GraphPad Prism Software).

Results

CSCs exhibit distinct actin dynamics and organization

The balance between F-actin and G-actin can function to drive cell fate decisions such as the maintenance of stem cell status and self-renewal versus differentiation (65). To determine the F/G actin ratio, we carried out flow cytometry in $CD24^{hi}CD44^{hi}$ CSCs vs. bulk tumor cells in low passage human xenografts. Although CSC populations have a higher baseline expression of both F-actin and G-actin, we found that these cells exhibit a lower relative amount of polymerized actin (Fig 1a), reminiscent of undifferentiated keratinocyte progenitors. We also wanted to characterize the organization of actin in CSCs and differentiated cells. We grew the xenografts as spheres in FBS free media to expand the CSC populations (63, 100), then differentiated tumor.spheres by culturing them in FBS-containing sphere media. To characterize the actin organization during CSC differentiation, we stained single cells with phalloidin and DNAse1 to visualize polymerized and free actin, respectively. CSCs were rounder and exhibited punctate cortical F-actin staining and a strong G-actin staining pattern, with presence of G-actin in the nucleus (Fig 1b). This G-actin staining pattern is characteristic of undifferentiated keratinocyte progenitors (65). In contrast, cells from differentiated spheres had a flattened morphology with a continuous cortical F-actin pattern and only a weak staining for G-actin. An increased amount of cortical is associated with the differentiation of MSCs towards the osteogenic lineage (70). Therefore CSCs display actin cytoskeletal features characteristic of undifferentiated cells in several normal systems.

Ezrin regulates actin dynamics

We decided to use Ezrin as a tool to study cytoskeletal dynamics for several reasons. Ezrin modulates cell shape and actin dynamics across multiple organisms. Additionally, Ezrin binds to the cytoplasmic tail of the CSC marker CD44, and this interaction is necessary for the signaling transduction cascade of another CSC marker, c-Met. We examined Ezrin expression in CSCs and differentiated tumor cells and found that CSCs from human xenografts and PDAC cell lines expressed higher amounts of Ezrin relative to non-CSCs (fig 2a). Ezrin is activated by phopsphorylation after which it binds to actin and we found that CSCs express highel levels of pERM and actin binding (Fig 2a).

We knocked down Ezrin in L3.6pl cells using an inducible shRNA and found that loss of Ezrin increased cortical F-actin and the F/G actin ratio, decreased nuclear G-actin staining, and caused a flattened morphology, consistent with changes during CSC differentiation. (Fig 2b,c, Sup 1). Our findings indicate that Ezrin is a CSC associated protein and regulates actin dynamics.

Ezrin regulates CSC functions

To determine the impact of Ezrin loss on functional properties we knocked down Ezrin for seven days in L3.6pl, E3LZ10.7, and MIA PaCa-2 cells. Ezrin is a well-documented regulator of motility in several malignancies, including pancreatic cancer (96, 97). As expected, the total number of migratory cells in all cell lines was decreased after 7 days of Ezrin shRNA induction (fig. 3a, Sup 3).

To quantify clonogenic growth potential we withdrew the doxycycline after 7 days of doxycycline treatment and plated a proportion of the remaining cells in a semi-solid colony formation media. Loss of Ezrin expression for 7 days resulted in a decrease in the total clonogenic output of the cells (Fig 3b. sup 3). To quantify self-renewal, we serially re-plated the remaining colonies and found a decrease in the total clonogenic output over two serial replatings in all cell lines (Fig 3b, Sup 3). Even though doxycycline administration was discontinued during colony formation, the cells never regained their ability to form colonies during the 28 days in colony formation media. When loss of Ezrin was induced over a period of 21 days, L3.6pl cells regained mRNA expression, however, they never recovered their self-renewal potential (Sup 2). Our results indicate that the change in actin dynamics over 7 days led to a permanent loss of self-renewal potential. Moreover, at the end of the 7 day treatment there were no significant changes in the viability of L3.6pl cells (Fig 3c). We also characterized the changes that occur earlier after Ezrin loss, and foud that 72 hours of doxycycline treatment did not significantly increase apoptosis (Fig 3c).

We wanted to know whether these changes could be due to a loss of CSC frequency. When we assessed for CSCs by flow cytometry after 7 days of shRNA loss, we say a decrease in $CD24^{+}CD44^{+}$, $CD44^{+}cMet^{+}$ (Fig 3d). Interestingly, although the cells did not express CD133, loss of Ezrin decreased the frequency of additional CSC phenotypes, such as $ALDH^{+}$ cells (sup 2).

In order to determine the relationship between actin dynamics and clonogenic tumor growth we inhibited actin polymerization with CytochalasinD and Y-27632 in L3.6pl cells over period of 24 hours. CytochalasindD disrupts F-actin filaments and

inhibits polymerization, whereas Y-27632 can indirectly lead to an increase in depolymerization (101-103). We observed an increase in colony formation potential following treatment with both drugs (Sup 2).

We also expressed a constitutively active form of Ezrin with a threonine to aspartic acid substitution at residue 567 (t567d) in L3.6pl cells and observed increased Ezrin activation, accompanied by an increase in migratory cells, clonogenicity, and the frequency of CSCs (Fig 3 e, f, g, Sup 4).

Loss of Ezrin expression diminishes in vitro tumorigenicity

CSCs are functionally defined by their enhanced tumor formation potential and we extended our *in vitro* findings by examining tumor formation *in vivo*. We injected L3.6pl cells containing doxycycline inducible shRNA against Ezrin or a control shRNA subcutaneously into NSG mice, and following formation of primary tumors treated mice with doxycycline (fig 4a). During doxycycline treatment, there were no significant changes in tumor sizes, although, histologically loss of Ezrin resulted in more clusters of differentiation in the primary tumors (Fig 4b,c). We then collected tumors and re-transplanted decreasing numbers of tumor cells into naïve recipients. In the absence of additional doxycycline treatment, the tumor initiating frequency during secondary engraftment of cells carrying the Ezrin shRNA construct was significantly decreased compared to cells with the control shRNA (Table 2). There were no differences in tumor growth and clonogenicity between the two groups when doxycycline was not administered (sup 5). Thus, transient Ezrin knockdown impairs long-term clonogenic growth and self-renewal *in vivo*.

Pharmacological inhibition of Ezrin activity decreases the self-renewal capacity in human pancreatic cancer samples

Recently we identified several compounds that that inhibit the phosphorylation of Ezrin at threonine 567 and its interaction with actin (84). These compounds blocked Ezrin-mediated invasion of cell monolayers and survival of osteosarcoma cells in a mouse lung-culture system. We tested one of the compounds (Drug8) in PDAC cells and found that it inhibited the binding of Ezrin to actin and decreased both colony formation and migration of L3.6pl, E3Lz 10.7, and MIA PaCa-2 cells (Fig 5a, Sup 6). We also treated tumor spheres generated from low passage tumor xenografts with Drug 8. In three distinct clinical specimens sphere formation was significantly inhibited (Fig 5b). Therefore, pharmacological inhibition of Ezrin may represent a novel strategy to target pancreatic CSCs.

Ezrin regulates actin dynamics by antagonizing RhoA activity

Ezrin is an orthologue of the *Drosophila* Moesin, which maintains cellular morphology by antagonizing the activity of the small GTPase Rho (104). In this context loss of Rho activity can rescue the defects associated with loss of Moesin completely. In mammalian systems RhoA activity is increased with the loss Ezrin and inhibition of the GTPase rescues defects in neuritogenesis and axonal growth in cultured cortical neurons of Ezrin knockout mice (76, 105). RhoA typically regulates actin polymerization through its effector Rho-associated protein kinase (ROCK), and ROCK activation leads to inhibition of actin depolymerization (102). ROCK activity plays a role in both normal and cancer stem cell biology. In normal systems cell fate decision based on cell shape

changes are regulated by the balance of actin polymerization, and modulation of RhoA activity and ROCK signaling (65, 69). Furthermore, inhibition of ROCK, leads to the expansion of colorectal cancer and glioblastoma CSCs (106, 107). To determine whether in PDAC Ezrin maintains a CSC-associated actin state we inhibited ROCK signaling with Y-27632, a specific inhibitor that competes with ATP for binding to the enzyme's catalytic site (103).

We knocked down Ezrin by shRNA, then treated with Y-27632 together with doxycycline for the remaining 48 hours, for a total of 72 hours. ROCK inhibition blocked the loss of clonogenicity, induced by Ezrin knockdown (Fig 6b). Thus Ezrin maintains CSCs, at least in part, by regulating actin polymerization through ROCK inhibition.

Discussion

Our results identify actin polymerization and organization as a novel mechanism for the regulation of CSCs. There are numerous mechanisms through which this process could occur. The balance between free and polymerized actin can influence transcriptional activity by regulating the availability of different co-factors (65). Presumably CSCs are able to self –renew and generate the bulk of the tumor by undergoing asymmetrical divisions. Cytoskeletal changes could regulate the balance between symmetric and asymmetric divisions by controlling cellular polarity (108). Alternatively, actin dynamics could serve to organize different membrane domains, and thus modulate activity of various cell surface receptors (109, 110). A further examination of the mechanisms of CSC regulation by the cytoskeleton would yield more targets for therapeutic intervention.

Small molecules that directly bind to actin and affect its polymerization have been widely used in experimental systems, and their activity can induce changes in cell fate in several contexts (65, 69). However, they lack specificity to a particular type of actin, and their potential effect on cardiac and skeletal muscle actin fibers precludes their use in the clinic (101). A way to safely modulate actin dynamics would be to target molecules associated with actin that are selectively upregulated in cancers. For examples tropomyosin is a core component of actin filaments. Different isoforms of tropomyosin exist and it is possible to affect actin filament compartments in cancer cells specifically, based on their tropomyosin isoform composition (111). We took advantage of the fact that Ezrin, a known regulator of actin polymerization, is expressed in multiple types of cancers, but not in the normal tissue of origin of tumors (85-92). Pharmacological

inhibition of Ezrin function allowed us to decrease the self-renewal potential of samples derived from human tumor xenogratfs. Thus, targeting Ezrin through small molecule inhibitors has the potential to improve clinical outcome in multiple cancers and recently a screen of the Medicines for Malaria Venture Malaria Box uncovered a compound with potent anti-Ezrin activity and a favorable drug-likeness profile (112).

Importantly, we demonstrate that maintaining stemness through regulation of actin polymerization is a mechanism common to several pancreatic CSCs phenotypes. Upon loss of Ezrin expression we observed a decrease in the frequency of $CD24^{+}CD44^{+}$, $CD44^{+}cMet^{+}$, and $ALDH^{+}$ phenotypes. When we over activated the protein, the increase in CSC functions was accompanied by an increase in the frequency of CSC phenotypes. One potential barrier to the successful elimination of CSCs in pancreatic tumors is the existing phenotypic diversity. Several pancreatic cancer CSC populations exist and the precise relationship between all of them is not completely characterized. Studies to eliminate pancreatic CSCs have focused on targeting cell surface receptors of or signaling pathways active in some of theses populations and to date no study has demonstrated the elimination of more than two populations (13, 25, 56, 58, 59, 64, 113-115). Our findings suggest that maintaining cell shape is a process fundamental to at least three CSC phenotypes, and thus targeting actin dynamics could lead to a successful elimination of all sources of self-renewal in the tumor.

Our observations could also be used to explain in part the role of desmoplasia in pancreatic cancer. The large deposition of extracellular matrix in pancreatic tumors would create a large compressive force and would also limit the space for cellular growth. These forces could cause changes in cellular shape and cytoskeletal organization, leading

to a loss of stemness. A similar mechanism functions in the developing skeleton. A rigid perichondrial membrane surrounds the primitive cartilage. Loss of this membrane results in unregulated growth in that tissue, most likely by allowing expansion of chondrocytic progenitors, rather then their differentiation into cartilage (116-118). The collapse of stroma in mouse models of PDAC leads to an accelerated disease with a less differentiated phenotype, and an increase in the frequency of tumor initiating cells (119, 120). Thus, the ability to maintain a particular actin filament organization in the face of restrictive pressure from the stroma might be critical for stem cell maintenance and our observations corroborate this hypothesis.

Elucidation of the role of these processes will inform better therapeutic developments. Our work demonstrates that actin cytoskeletal dynamics are a fundamental regulator of differentiation not only in normal systems, but also in CSCs. Manipulating actin polymerization and organization will improve clinical outcomes, by targeting the self-renewal potential of tumors.

Figure legends

Table 1.

Pancreatic CSC specific targeting strategies and agents

Figure 1

Actin cytoskeletal features of CSCs from human tumors. **A,** the ratio of filamentous (F-actin) to free (G-actin) in CSCs from low passage tumor xenografts measured by flow cytometry. **B,** the organization of F-actin and G-actin in CSC-enriched and differentiated spheres derived from low passage human xenografts assessed by phalloidin and DNAse1 staining (60X magnification)

Figure 2

Effect of Ezrin knockdown on actin cytoskeletal organization. **A,** Ezrin and pERM expression in CSCs from a low passage human xenograft (Panc 265) and a human PDAC cell lines (L3.6pl, E3LZ 10.7). **B,** total F-actin and total G-actin in L3.6pl cells after Ezrin knockdown. **C,** filamentous actin organization in L3.6pl cells after Ezrin knockdown. * represents $P<0.05$, **$P<0.01$ after one sample t test. n.s represents non-significant after one sample t test

Figure 3.

Effects of Ezrin knockdown and over activation in L3.6pl cells. **A,** migratory output after seven days of Ezrin knockdown. **B,** relative clonogenic output upon serial re-

plating after seven days of Ezrin knockdown. **C,** Annexin V staining of three and seven days after Ezrin knockdown. **D,** the frequency of CSC populations after seven days of Ezrin knockdown. **E, F, G**, clonogenic (E) and migratory (F) output and CSC frequency (G) after three days of Ezrin t567d mutant expression. * represents $P<0.05$, ** $P<0.01$, *** $P<0.001$ after one sample t test (A B, E, F). * represents $P<0.05$ after Student's t test (D)

Figure 4.

In vivo inhibition of Ezrin expression in L3.6pl cells. **A,** experimental design; control or Ezrin shRNA tumors were allowed to establish, and shRNA expression was induced for 9 days, after which the tumors were re-transplanted without further shRNA induction. **B,** tumor growth and Ezrin mRNA levels in primary tumors. C, histological characteristics of primary tumors (n=4 tumors in each group)

Table 2.

Tumor initiation in naïve secondary recipients.

Figure 5.

Pharmacological inhibition of Ezrin. **A,** clonogenicity, migratory output, and cell viability after three days of Drug 8 treatment (1uM) in L3.6pl cells. **B,** secondary sphere formation of low passage xenograft–derived spheres (Panc 265, Panc 185, JH 102) after three days of drug 8 treatment (1uM). * represents $P<0.05$, ** $P<0.01$ after one sample t test

Figure 6.

Ezrin regulates CSC functions by antagonizing ROCK signaling. Clonogenic output in L3.6pl cells after three days of Ezrin knockdown accompanied by ROCK inhibition. ** represents $p<0.01$, ** $p<0.001$ after Student's t test. n.s. represents not significant

Supplemental figure 1.

Generation of L3.6pl knockdown cells. mRNA levels (left panel) and protein expression (right panel) after seven days of Ezrin knockdown.

Supplemental figure 2.

Effect of Ezrin knockdown in L3.6pl cells. A, Ezrin mRNA levels (left panel) and clonogenicity (right panel) of L3.6pl cells after 21 days of Ezrin knockdown. B, frequency of ALDH+ CSCs after three days of Ezrin knockdown. C, clonogenicity after inhibition of actin polymerization for 24 hours in L3.6pl cells. L3.6pl cells containing a control shRNA construct were treated with doxycycline for 24 hours together either Cytochalasin D (left panel) of Y-27632 (right panel). ** represents P,0.01, ***$p<0.001$ after one sample t test.

Supplemental figure 3.

Effects of Ezrin knockdown in E3LZ 10.7 and MIA PaCa-2 cells. Functional consequences of Ezrin knockdown in E3LZ1 10.7 cells (A) and MIA PaCa-2 cells (B). Clonogenicity and self-renewal (top panel), total migratory output (middle panel),

and Ezrin mRNA levels (bottom panel) after seven days of Ezrin knockdown. ** represents $p<0.01$, ***$p<0.001$ after one sample t test.

Supplemental figure 4.

Generation of L3.6pl cells containing overactive Ezrin mutant. L3.6pl cells transduced with an empty pInducer20 vector (empty) or a vector with a threonine 567 to aspartic acid substitution (t567d) of Ezrin cDNA. Expression of the construct was induced for three days with doxycycline, after which a pull-down with an Ezrin antibody and blotting for Ezrin, pERM, and actin was performed.

Supplemental figure 5.

In vivo knockdown of Ezrin. Clonogeicity of induced (top left panel) and uninduced (top right panel) L3.6pl tumors containing control and Ezrin shRNA constructs. Tumor volumes of uninduced L3.6pl tumors containing control and Ezrin shRNA constructs (bottom right panel; n=4 tumors in each group)

Supplemental figure 6.

Pharmacological inhibition of Ezrin. Clonogenicity (top panel) and total migratory output (bottom panel) in E3LZ 10.7 (A) and MIA PaCa-2 (B) cells after three days of Drug 8 treatment (1uM). ** represents $p<0.01$ after one sample t test.

Figures and tables

Table1. Targeting of pancreatic cancer stem cells

Study	Target receptor/pathway	Target population	Agent
Li *et al*.(25)	c-Met	c-Met^{high}CD44^{+} CD44^{+}CD24^{+}ESA^{+}	XL184
Rajeshkumar *et al*.(115)	DR5	ALDH^{+} CD44^{+}CD24^{+}ESA^{+}	DR5 Agonistic monoclonal antibody
Lonardo *et al(58)*	ALK4	CD133^{+}	SB431542
Jimeno *et al*.(13) Feldmann *et al*.(114) Feldmann *et al*.(59)	Hedgehog	ALDH^{+} CD44^{+}CD24^{+}ESA^{+}	Cyclopamine, IPI269609
Mullendore *et al*.(62)	Notch	ALDH^{+}	GSI-18
Zhang *et al*.(113)	EMT	CD133^{+}	Salinomycin
Balic *et al*. (121)	CXCR4, Hedgehog	CD133^{+}	Chloroquine
Cioffi *et al.(56)*	CD47	CD133^{+}	CD47 Antagonistic monoclonal antibody
Lonardo *et al.* (122) Sancho *et al.(63)*	OXPHOS	CD133^{+}	Metformin JQ-1

Figure 1

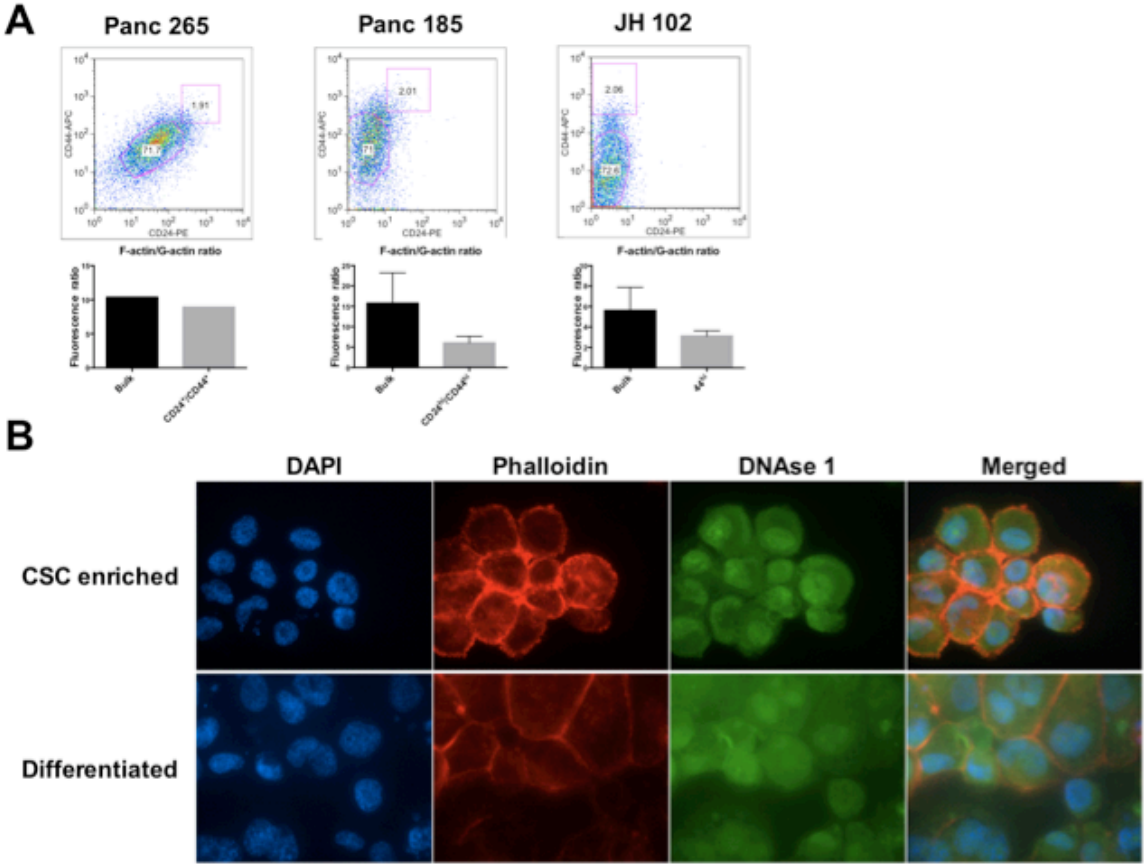
A
Panc 265
Panc 185
JH 102
CD44-APC
CD24-PE
1.91
71.7
2.01
71
2.06
72.6
F-actin/G-actin ratio
Fluorescence ratio
Bulk
B
DAPI
Phalloidin
DNAse 1
Merged
CSC enriched
Differentiated

Figure 2

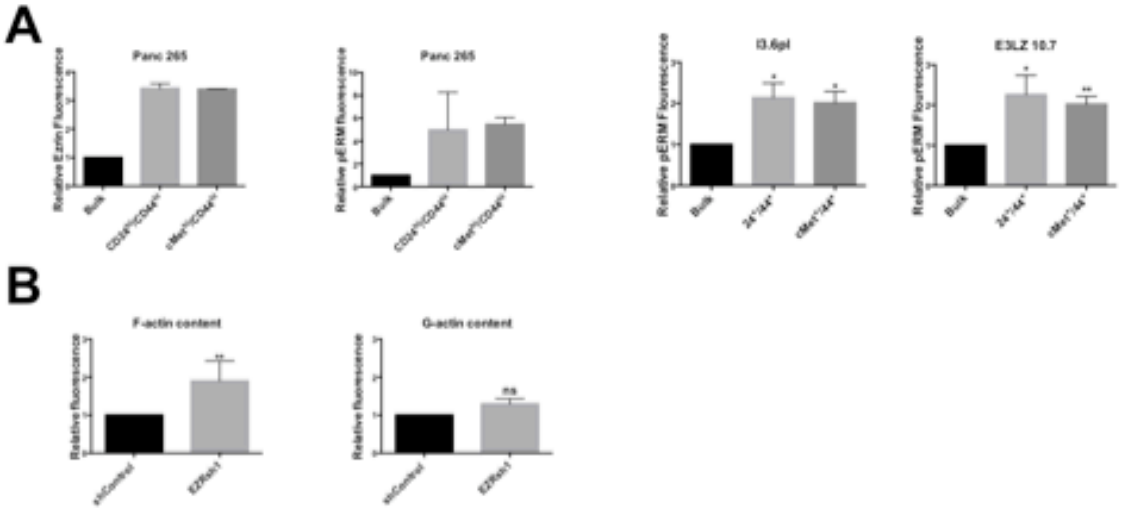
A
Panc 265
Relative Ezrin Fluorescence
Bulk
Panc 265
Relative pERM fluorescence
Bulk
I3.6pl
Relative pERM Flourescence
Bulk
E3LZ 10.7
Relative pERM Flourescence
Bulk
B
F-actin content
Relative fluorescence
shControl
EZRsh1
G-actin content
Relative fluorescence
ns
shControl
EZRsh1

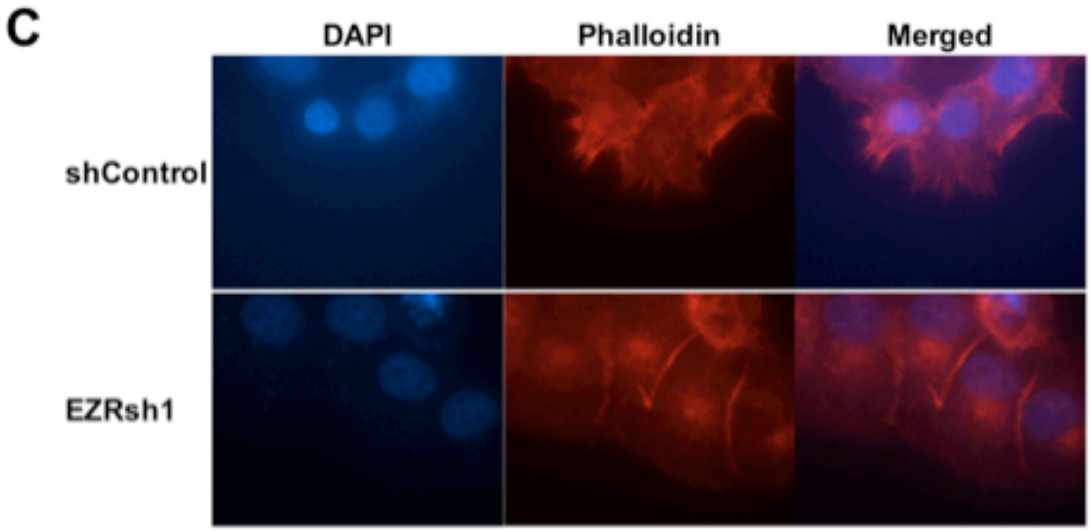
C
DAPI
Phalloidin
Merged
shControl
EZRsh1

Figure 3

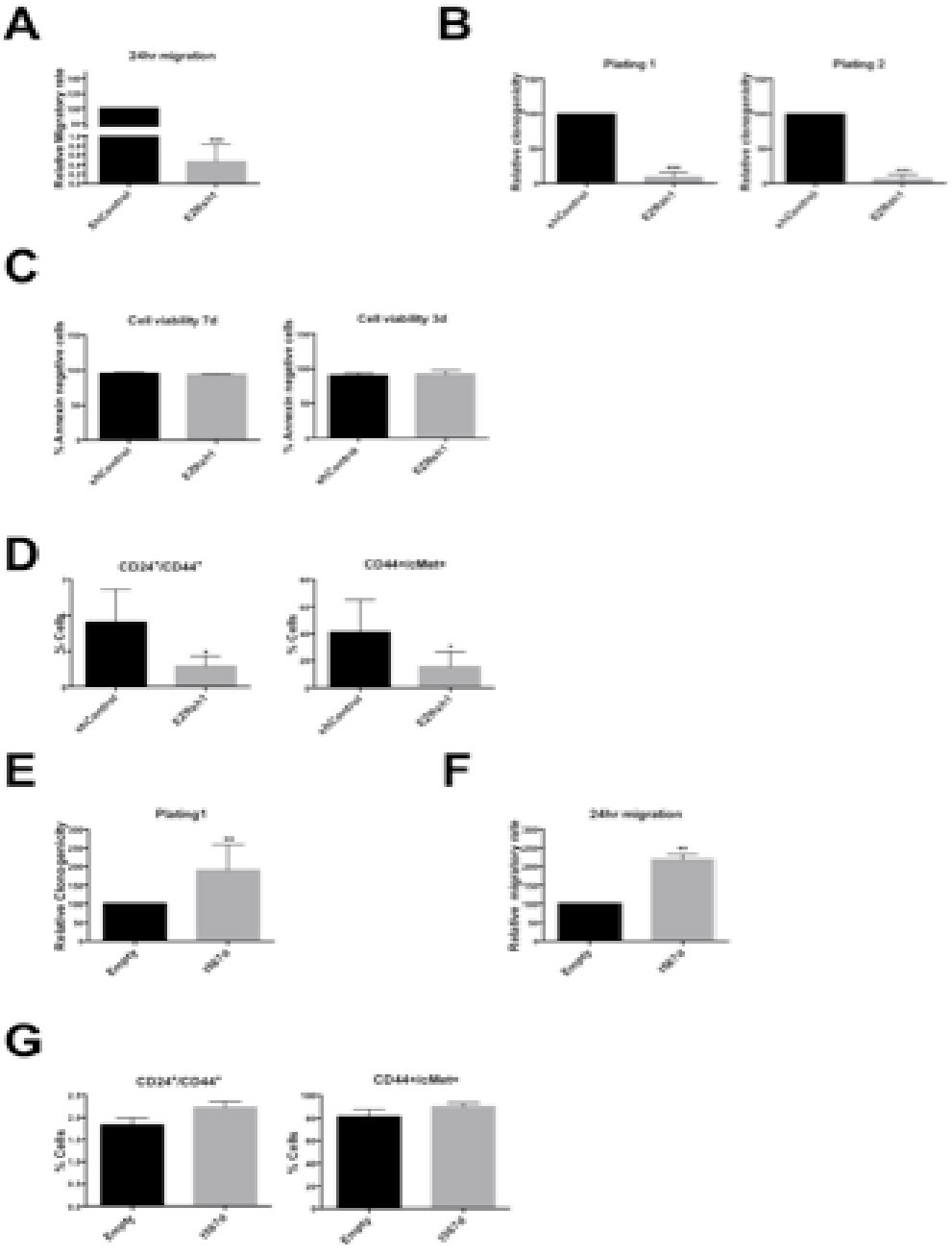
A
24hr migration
Relative Migratory rate
B
Plating 1
Plating 2
Relative clonogenicity
C
Cell viability 7d
Cell viability 3d
% Annexin negative cells
D
CD24+/CD44+
CD44+/cMet+
% Cells
E
Plating1
Relative Clonogenicity
F
24hr migration
Relative migratory rate
G
CD24+/CD44+
CD44+/cMet+
% Cells

Figure 4

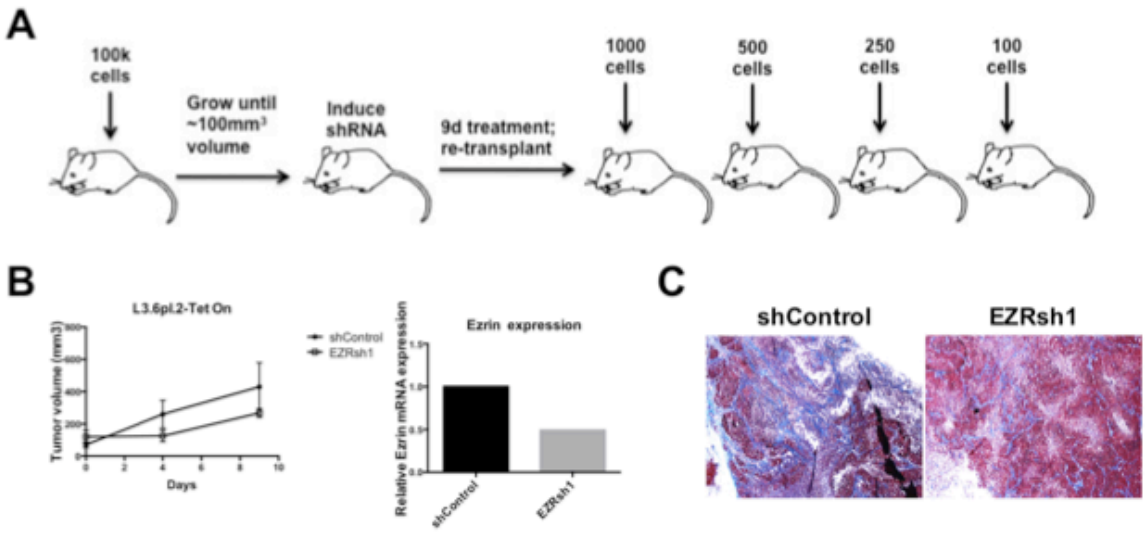

Table 2

Tumor initiating frequency 30d post re-transplant:

	1000 cells	500 cells	250 cells	100 cells	p-value
shControl	8/8	12/12	12/12	4/4	
EZRsh1	7/8	11/12	5/12	2/4	2.1*10^-6

Figure 5

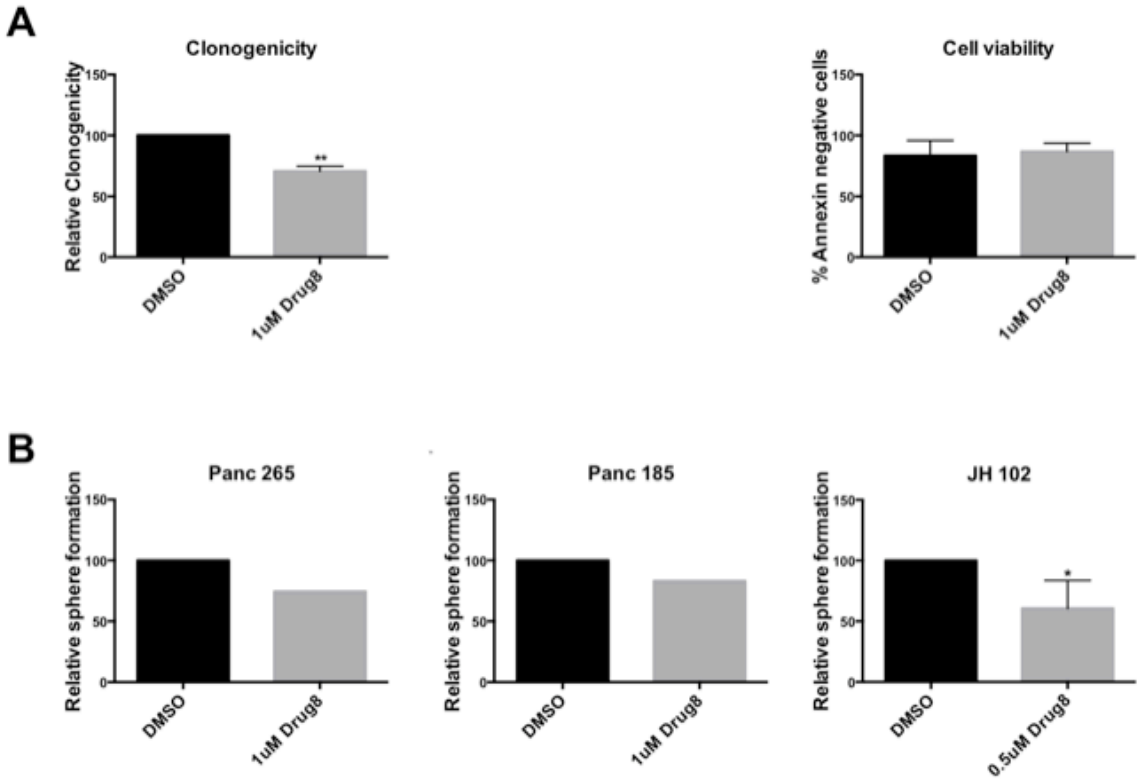

Figure 6

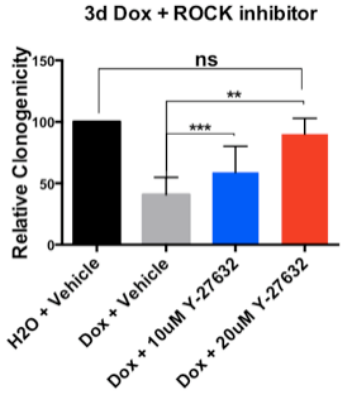

Supplemental fig. 1

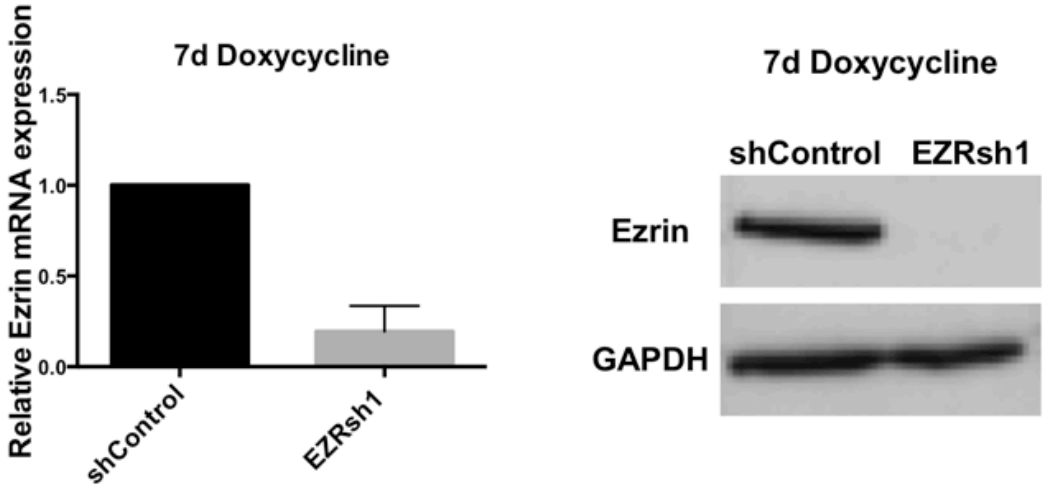

Supplemental fig. 2

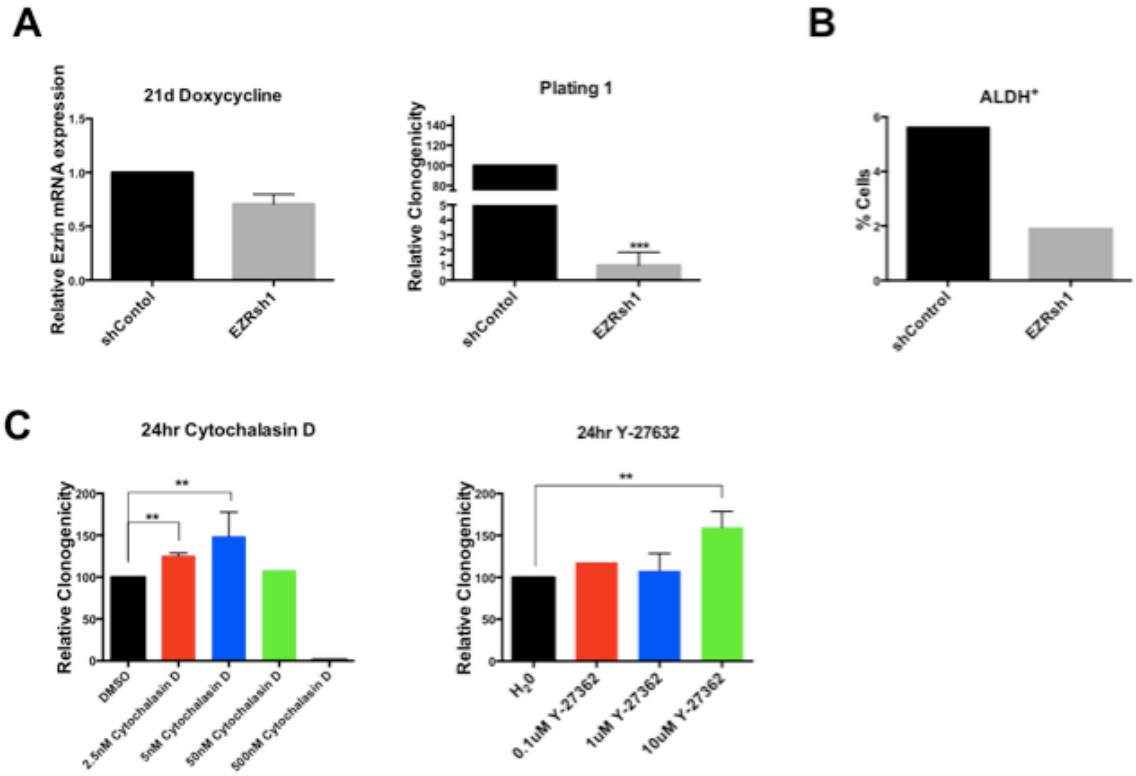

Supplemental fig. 3

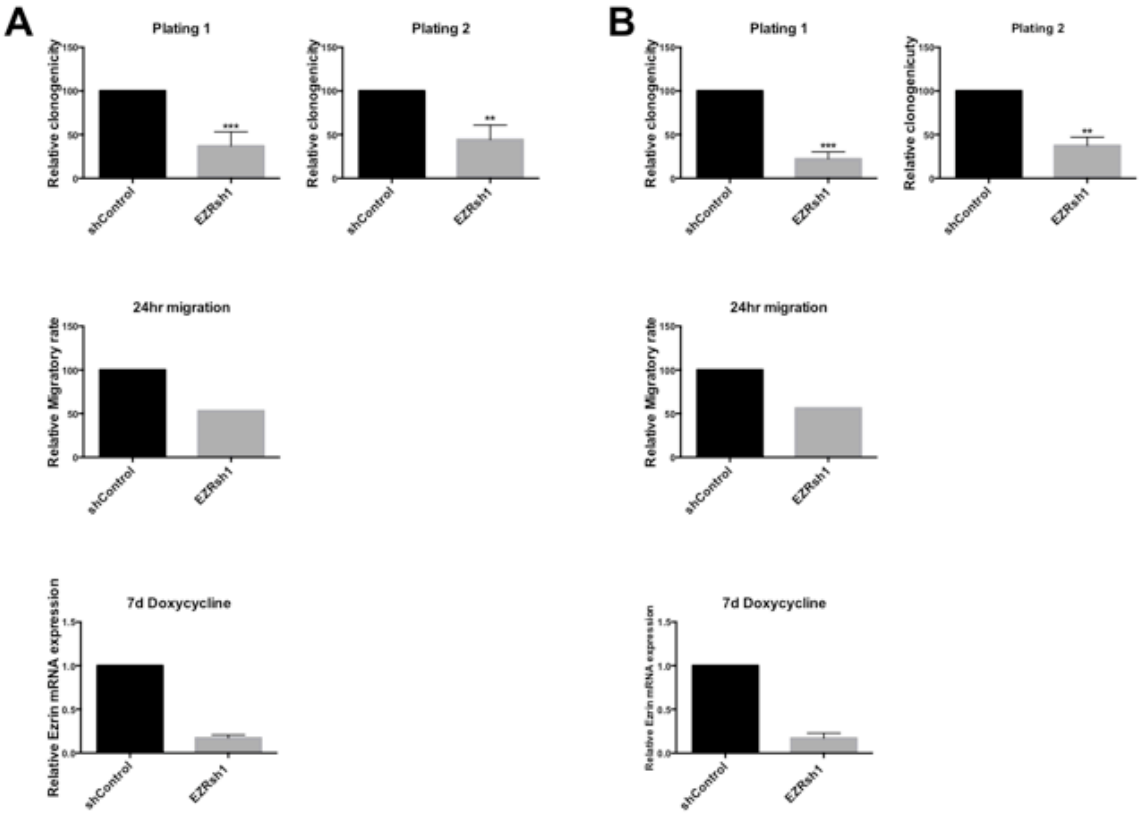

Supplemental fig. 4

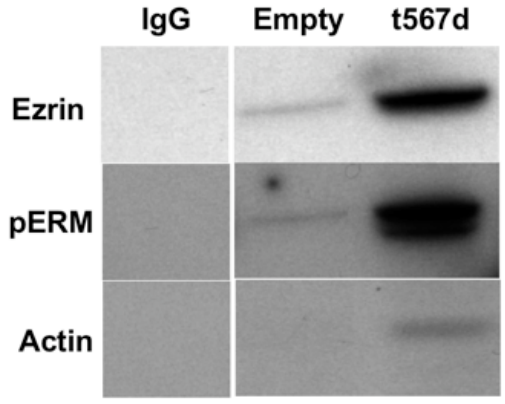

Supplemental fig. 5

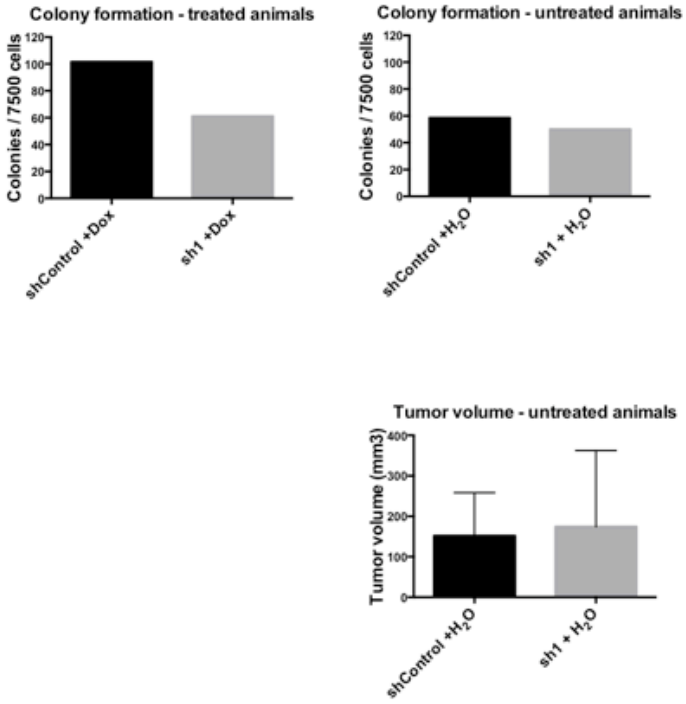

Supplemental fig. 6

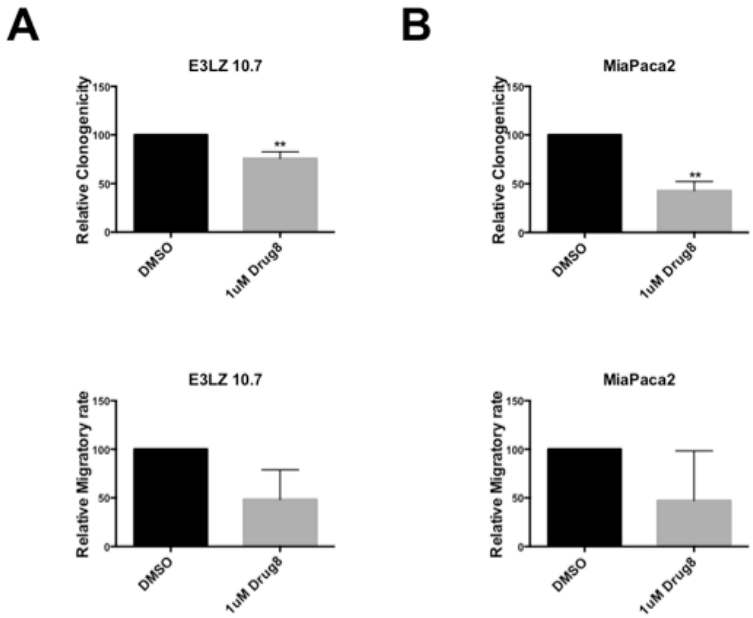

Bibliography

1. Siegel RL, Miller KD, Jemal A. Cancer statistics, 2016. CA: a cancer journal for clinicians. 2016;66:7-30.

2. Reya T, Morrison SJ, Clarke MF, Weissman IL. Stem cells, cancer, and cancer stem cells. Nature. 2001;414:105-11.

3. Bonnet D, Dick JE. Human acute myeloid leukemia is organized as a hierarchy that originates from a primitive hematopoietic cell. Nature medicine. 1997;3:730-7.

4. Lapidot T, Sirard C, Vormoor J, Murdoch B, Hoang T, Caceres-Cortes J, et al. A cell initiating human acute myeloid leukaemia after transplantation into SCID mice. Nature. 1994;367:645-8.

5. Li C, Heidt DG, Dalerba P, Burant CF, Zhang L, Adsay V, et al. Identification of pancreatic cancer stem cells. Cancer Res. 2007;67:1030-7.

6. Rasheed ZA, Yang J, Wang Q, Kowalski J, Freed I, Murter C, et al. Prognostic significance of tumorigenic cells with mesenchymal features in pancreatic adenocarcinoma. Journal of the National Cancer Institute. 2010;102:340-51.

7. Hermann PC, Huber SL, Herrler T, Aicher A, Ellwart JW, Guba M, et al. Distinct populations of cancer stem cells determine tumor growth and metastatic activity in human pancreatic cancer. Cell Stem Cell. 2007;1:313-23.

8. Miranda-Lorenzo I, Dorado J, Lonardo E, Alcala S, Serrano AG, Clausell-Tormos J, et al. Intracellular autofluorescence: a biomarker for epithelial cancer stem cells. Nature methods. 2014;11:1161-9.

9. Li C, Wu JJ, Hynes M, Dosch J, Sarkar B, Welling TH, et al. c-Met is a marker of pancreatic cancer stem cells and therapeutic target. Gastroenterology. 2011;141:2218-27 e5.

10. Kern SE, Shibata D. The Fuzzy Math of Solid Tumor Stem Cells: A Perspective. Cancer research. 2007;67:8985-8.

11. Adams JM, Strasser A. Is Tumor Growth Sustained by Rare Cancer Stem Cells or Dominant Clones? Cancer research. 2008;68:4018-21.

12. Tomasson MH. Cancer stem cells: A guide for skeptics. Journal of Cellular Biochemistry. 2009;106:745-9.

13. Jimeno A, Feldmann G, Suárez-Gauthier A, Rasheed Z, Solomon A, Zou G-M, et al. A direct pancreatic cancer xenograft model as a platform for cancer stem cell therapeutic development. Molecular cancer therapeutics. 2009;8:310-4.

14. Penchev VR, Rasheed ZA, Maitra A, Matsui W. Heterogeneity and targeting of pancreatic cancer stem cells. Clinical cancer research : an official journal of the American Association for Cancer Research. 2012;18:4277-84.

15. Clarke MF, Dick JE, Dirks PB, Eaves CJ, Jamieson CHM, Jones DL, et al. Cancer stem cells--perspectives on current status and future directions: AACR Workshop on cancer stem cells. Cancer research. 2006;66:9339-44.

16. Brennan S, Matsui W. Cancer stem cells: controversies in multiple myeloma. J Mol Med. 2009.

17. Lapidot T, Fajerman Y, Kollet O. Immune-deficient SCID and NOD/SCID mice models as functional assays for studying normal and malignant human hematopoiesis. Journal of Molecular Medicine. 1997;75:664-73.

18. Singh SK, Hawkins C, Clarke ID, Squire JA, Bayani J, Hide T, et al. Identification of human brain tumour initiating cells. Nature. 2004;432:396-401.

19. O'Brien CA, Pollett A, Gallinger S, Dick JE. A human colon cancer cell capable of initiating tumour growth in immunodeficient mice. Nature. 2007;445:106-10.

20. Matsui W, Wang Q, Barber JP, Brennan S, Smith BD, Borrello I, et al. Clonogenic multiple myeloma progenitors, stem cell properties, and drug resistance. Cancer research. 2008;68:190-7.

21. Ginestier C, Hur MH, Charafe-Jauffret E, Monville F, Dutcher J, Brown M, et al. ALDH1 Is a Marker of Normal and Malignant Human Mammary Stem Cells and a Predictor of Poor Clinical Outcome. Cell stem cell. 2007;1:555-67.

22. Jones RJ, Gocke CD, Kasamon YL, Miller CB, Perkins B, Barber JP, et al. Circulating clonotypic B cells in classic Hodgkin lymphoma. Blood. 2009;113:5920-6.

23. Al-Hajj M, Wicha MS, Benito-Hernandez A, Morrison SJ, Clarke MF. Prospective identification of tumorigenic breast cancer cells. Proc Natl Acad Sci USA. 2003;100:3983-8.

24. Dalerba P, Dylla SJ, Park I-K, Liu R, Wang X, Cho RW, et al. Phenotypic characterization of human colorectal cancer stem cells. Proc Natl Acad Sci USA. 2007;104:10158-63.

25. Li C, Wu JÄ, Hynes M, Dosch J, Sarkar B, Welling TH, et al. c-Met Is a Marker of Pancreatic Cancer Stem Cells and Therapeutic Target. Gastroenterology. 2011;141:2218-27.e5.

26. Emadi A, Jones RJ, Brodsky RA. Cyclophosphamide and cancer: golden anniversary. Nat Rev Clin Oncol. 2009;6:638-47.

27. Rovira M, Scott S-G, Liss AS, Jensen J, Thayer SP, Leach SD. Isolation and characterization of centroacinar/terminal ductal progenitor cells in adult mouse pancreas. Proc Natl Acad Sci USA. 2009.

28. Ishizawa K, Rasheed ZA, Karisch R, Wang Q, Kowalski J, Susky E, et al. Tumor-initiating cells are rare in many human tumors. Cell stem cell. 2010;7:279-82.

29. Li Y, Li A, Glas M, Lal B, Ying M, Sang Y, et al. c-Met signaling induces a reprogramming network and supports the glioblastoma stem-like phenotype. Proceedings of the National Academy of Sciences. 2011;108:9951-6.

30. Li C, Heidt DG, Dalerba P, Burant CF, Zhang L, Adsay V, et al. Identification of pancreatic cancer stem cells. Cancer research. 2007;67:1030-7.

31. Rasheed ZA, Yang J, Wang Q, Kowalski J, Freed I, Murter C, et al. Prognostic significance of tumorigenic cells with mesenchymal features in pancreatic adenocarcinoma. Journal of the National Cancer Institute. 2010;102:340-51.

32. Kim MP, Fleming JB, Wang H, Abbruzzese JL, Choi W, Kopetz S, et al. ALDH Activity Selectively Defines an Enhanced Tumor-Initiating Cell Population Relative to CD133 Expression in Human Pancreatic Adenocarcinoma. PloS one. 2011;6:e20636.

33. Rasheed ZA, Kowalski J, Smith BD, Matsui W. Concise review: Emerging concepts in clinical targeting of cancer stem cells. Stem cells. 2011;29:883-7.

34. Feig C, Gopinathan A, Neesse A, Chan D, Cook N, Tuveson DA. The pancreas cancer microenvironment. Clinical cancer research : an official journal of the American Association for Cancer Research. 2012;18:XX-XX.

35. Bar EE, Lin A, Mahairaki V, Matsui W, Eberhart CG. Hypoxia increases the expression of stem-cell markers and promotes clonogenicity in glioblastoma neurospheres. American Journal Of Pathology. 2010.

36. Le A, Rajeshkumar N, Maitra A, Dang CV. Conceptual framework for cutting the pancreatic cancer fuel supply. Clinical cancer research : an official journal of the American Association for Cancer Research. 2012;18:XX-XX.

37. Gupta PB, Onder TT, Jiang G, Tao K, Kuperwasser C, Weinberg RA, et al. Identification of selective inhibitors of cancer stem cells by high-throughput screening. Cell. 2009;138:645-59.

38. Mani S, Evans K, Hollier B, Guo W, Weinberg R. Generation of Stem-like Cells via EMT: A New Twist in Cancer Initiation and Progression. AACR Education Book. 2009;2009:173.

39. Wellner U, Schubert J, Burk UC, Schmalhofer O, Zhu F, Sonntag A, et al. The EMT-activator ZEB1 promotes tumorigenicity by repressing stemness-inhibiting microRNAs. Nat Cell Biol. 2009;11:1487-95.

40. Maitra A, Adsay NV, Argani P, Iacobuzio-Donahue C, De MA, Cameron JL, et al. Multicomponent analysis of the pancreatic adenocarcinoma progression model using a pancreatic intraepithelial neoplasia tissue microarray. ModPathol. 2003;16:902-12.

41. Hruban RH, van Mansfeld AD, Offerhaus GJ, van Weering DH, Allison DC, Goodman SN, et al. K-ras oncogene activation in adenocarcinoma of the human pancreas. A study of 82 carcinomas using a combination of mutant-enriched polymerase chain reaction analysis and allele-specific oligonucleotide hybridization. American Journal of Pathology. 1993;143:545-54.

42. Redston MS, Caldas C, Seymour AB, Hruban RH, da Costa L, Yeo CJ, et al. p53 Mutations in Pancreatic Carcinoma and Evidence of Common Involvement of Homocopolymer Tracts in DNA Microdeletions. Cancer research. 1994;54:3025-33.

43. Hahn SA, Schutte M, Hoque ATMS, Moskaluk CA, da Costa LT, Rozenblum E, et al. DPC4, A Candidate Tumor Suppressor Gene at Human Chromosome 18q21.1. Science. 1996;271:350-3.

44. Jones S, Zhang X, Parsons DW, Lin JC-H, Leary RJ, Angenendt P, et al. Core signaling pathways in human pancreatic cancers revealed by global genomic analyses. Science. 2008;321:1801-6.

45. Tuveson DA, Hingorani SR. Ductal Pancreatic Cancer in Humans and Mice. Cold Spring Harbor Symposia on Quantitative Biology. 2005;70:65-72.

46. Anderson K, Lutz C, van Delft FW, Bateman CM, Guo Y, Colman SM, et al. Genetic variegation of clonal architecture and propagating cells in leukaemia. Nature. 2011;469:356-61.

47. Notta F, Mullighan CG, Wang JCY, Poeppl A, Doulatov S, Phillips LA, et al. Evolution of human BCR-ABL1 lymphoblastic leukaemia-initiating cells. Nature. 2011;469:362-7.

48. Yachida S, Jones S, Bozic I, Antal T, Leary R, Fu B, et al. Distant metastasis occurs late during the genetic evolution of pancreatic cancer. Nature. 2010;467:1114-7.

49. Gerlinger M, Rowan AJ, Horswell S, Larkin J, Endesfelder D, Gronroos E, et al. Intratumor Heterogeneity and Branched Evolution Revealed by Multiregion Sequencing. New England Journal of Medicine. 2012;366:883-92.

50. Maitra A, Kern SE, Hruban RH. Molecular pathogenesis of pancreatic cancer. Best PractRes Clin Gastroenterol. 2006;20:211-26.

51. Greaves M, Maley CC. Clonal evolution in cancer. Nature. 2012;481:306-13.

52. Iacobuzio-Donahue C, Velculescu V, Wolfgang C, Hruban RH. The genetic basis of pancreas cancer development and progression: insights from whole-exome and whole-genome sequencing. Clinical cancer research : an official journal of the American Association for Cancer Research. 2012;18:XX-XX.

53. Cioffi M, Dorado J, Baeuerle PA, Heeschen C. EpCAM/CD3-Bispecific T-cell Engaging Antibody MT110 Eliminates Primary Human Pancreatic Cancer Stem Cells. Clin Cancer Res. 2012;18:465-74.

54. Dalerba P, Cho RW, Clarke MF. Cancer stem cells: models and concepts. Annu Rev Med. 2007;58:267-84.

55. Jin L, Hope KJ, Zhai Q, Smadja-Joffe F, Dick JE. Targeting of CD44 eradicates human acute myeloid leukemic stem cells. Nature medicine. 2006;12:1167-74.

56. Cioffi M, Trabulo S, Hidalgo M, Costello E, Greenhalf W, Erkan M, et al. Inhibition of CD47 Effectively Targets Pancreatic Cancer Stem Cells via Dual Mechanisms. Clinical cancer research : an official journal of the American Association for Cancer Research. 2015;21:2325-37.

57. Rajeshkumar NV, Rasheed ZA, Garcia-Garcia E, Lopez-Rios F, Fujiwara K, Matsui WH, et al. A combination of DR5 agonistic monoclonal antibody with gemcitabine targets pancreatic cancer stem cells and results in long-term disease control in human pancreatic cancer model. Mol Cancer Ther. 2010;9:2582-92.

58. Lonardo E, Hermann PC, Mueller M-T, Huber S, Balic A, Miranda-Lorenzo I, et al. Nodal/Activin Signaling Drives Self-Renewal and Tumorigenicity of Pancreatic Cancer Stem Cells and Provides a Target for Combined Drug Therapy. Cell stem cell. 2011;9:433-46.

59. Feldmann G, Fendrich V, McGovern K, Bedja D, Bisht S, Alvarez H, et al. An orally bioavailable small-molecule inhibitor of Hedgehog signaling inhibits tumor initiation and metastasis in pancreatic cancer. Molecular cancer therapeutics. 2008;7:2725-35.

60. Feldmann G, Dhara S, Fendrich V, Bedja D, Beaty R, Mullendore M, et al. Blockade of hedgehog signaling inhibits pancreatic cancer invasion and metastases: a new paradigm for combination therapy in solid cancers. Cancer Res. 2007;67:2187-96.

61. Olive KP, Jacobetz MA, Davidson CJ, Gopinathan A, McIntyre D, Honess D, et al. Inhibition of Hedgehog signaling enhances delivery of chemotherapy in a mouse model of pancreatic cancer. Science. 2009;324:1457-61.

62. Mullendore ME, Koorstra J-B, Li Y-M, Offerhaus GJ, Fan X, Henderson CM, et al. Ligand-dependent Notch signaling is involved in tumor initiation and tumor maintenance in pancreatic cancer. Clinical cancer research : an official journal of the American Association for Cancer Research. 2009;15:2291-301.

63. Sancho P, Burgos-Ramos E, Tavera A, Bou Kheir T, Jagust P, Schoenhals M, et al. MYC/PGC-1alpha Balance Determines the Metabolic Phenotype and Plasticity of Pancreatic Cancer Stem Cells. Cell metabolism. 2015;22:590-605.

64. Zhang G-N, Liang Y, Zhou L-J, Chen S-P, Chen G, Zhang T-P, et al. Combination of salinomycin and gemcitabine eliminates pancreatic cancer cells. Cancer letters. 2011;313:137-44.

65. Connelly JT, Gautrot JE, Trappmann B, Tan DW, Donati G, Huck WT, et al. Actin and serum response factor transduce physical cues from the microenvironment to regulate epidermal stem cell fate decisions. Nature cell biology. 2010;12:711-8.

66. Chowdhury F, Na S, Li D, Poh YC, Tanaka TS, Wang F, et al. Material properties of the cell dictate stress-induced spreading and differentiation in embryonic stem cells. Nature materials. 2010;9:82-8.

67. Murray P, Prewitz M, Hopp I, Wells N, Zhang H, Cooper A, et al. The self-renewal of mouse embryonic stem cells is regulated by cell-substratum adhesion and cell spreading. The international journal of biochemistry & cell biology. 2013;45:2698-705.

68. Kilian KA, Bugarija B, Lahn BT, Mrksich M. Geometric cues for directing the differentiation of mesenchymal stem cells. Proceedings of the National Academy of Sciences of the United States of America. 2010;107:4872-7.

69. Rowena McBeath DMP, Celeste M. Nelson KB, Chen aCS. Cell Shape, Cytoskeletal Tension, and RhoA Regulate Stem Cell Lineage Commitment. Developmental Cell. 2004;6.

70. Sliogeryte K, Thorpe SD, Lee DA, Botto L, Knight MM. Stem cell differentiation increases membrane-actin adhesion regulating cell blebability, migration and mechanics. Scientific reports. 2014;4:7307.

71. Oh S, Brammer KS, Li YS, Teng D, Engler AJ, Chien S, et al. Stem cell fate dictated solely by altered nanotube dimension. Proceedings of the National Academy of Sciences of the United States of America. 2009;106:2130-5.

72. Arpin M, Chirivino D, Naba A, Zwaenepoel I. Emerging role for ERM proteins in cell adhesion and migration. Cell adhesion & migration. 2011;5:199-206.

73. Bretscher A, Reczek D, Berryman M. Ezrin: a protein requiring conformational activation to link microfilaments to the plasma membrane in the assembly of cell surface structures. Journal of cell science. 1997;110 (Pt 24):3011-8.

74. Gautreau A, Louvard D, Arpin M. Morphogenic effects of ezrin require a phosphorylation-induced transition from oligomers to monomers at the plasma membrane. The Journal of cell biology. 2000;150:193-203.

75. Wakayama Y, Miura K, Sabe H, Mochizuki N. EphrinA1-EphA2 signal induces compaction and polarization of Madin-Darby canine kidney cells by inactivating Ezrin through negative regulation of RhoA. The Journal of biological chemistry. 2011;286:44243-53.

76. Saotome I, Curto M, McClatchey AI. Ezrin is essential for epithelial organization and villus morphogenesis in the developing intestine. Dev Cell. 2004;6:855-64.

77. Heiska L, Melikova M, Zhao F, Saotome I, McClatchey AI, Carpen O. Ezrin is key regulator of Src-induced malignant phenotype in three-dimensional environment. Oncogene. 2011;30:4953-62.

78. Parisiadou L, Xie C, Cho HJ, Lin X, Gu XL, Long CX, et al. Phosphorylation of ezrin/radixin/moesin proteins by LRRK2 promotes the rearrangement of actin

cytoskeleton in neuronal morphogenesis. The Journal of neuroscience : the official journal of the Society for Neuroscience. 2009;29:13971-80.

79. Manchanda N, Lyubimova A, Ho HY, James MF, Gusella JF, Ramesh N, et al. The NF2 tumor suppressor Merlin and the ERM proteins interact with N-WASP and regulate its actin polymerization function. The Journal of biological chemistry. 2005;280:12517-22.

80. Tsukita S, Oishi K, Sato N, Sagara J, Kawai A, Tsukita S. ERM family members as molecular linkers between the cell surface glycoprotein CD44 and actin-based cytoskeletons. The Journal of cell biology. 1994;126:391-401.

81. Crepaldi T, Gautreau A, Comoglio PM, Louvard D, Arpin M. Ezrin is an effector of hepatocyte growth factor-mediated migration and morphogenesis in epithelial cells. The Journal of cell biology. 1997;138:423-34.

82. Orian-Rousseau V, Chen L, Sleeman JP, Herrlich P, Ponta H. CD44 is required for two consecutive steps in HGF/c-Met signaling. Genes & development. 2002;16:3074-86.

83. Orian-Rousseau V, Morrison H, Matzke A, Kastilan T, Pace G, Herrlich P, et al. Hepatocyte growth factor-induced Ras activation requires ERM proteins linked to both CD44v6 and F-actin. Molecular biology of the cell. 2007;18:76-83.

84. Bulut G, Hong SH, Chen K, Beauchamp EM, Rahim S, Kosturko GW, et al. Small molecule inhibitors of ezrin inhibit the invasive phenotype of osteosarcoma cells. Oncogene. 2012;31:269-81.

85. Kang YK, Hong SW, Lee H, Kim WH. Prognostic implications of ezrin expression in human hepatocellular carcinoma. Molecular carcinogenesis. 2010;49:798-804.

86. Kobel M, Langhammer T, Huttelmaier S, Schmitt WD, Kriese K, Dittmer J, et al. Ezrin expression is related to poor prognosis in FIGO stage I endometrioid carcinomas. Modern pathology : an official journal of the United States and Canadian Academy of Pathology, Inc. 2006;19:581-7.

87. Elzagheid A, Korkeila E, Bendardaf R, Buhmeida A, Heikkila S, Vaheri A, et al. Intense cytoplasmic ezrin immunoreactivity predicts poor survival in colorectal cancer. Human pathology. 2008;39:1737-43.

88. Weng WH, Ahlen J, Astrom K, Lui WO, Larsson C. Prognostic impact of immunohistochemical expression of ezrin in highly malignant soft tissue sarcomas. Clinical cancer research : an official journal of the American Association for Cancer Research. 2005;11:6198-204.

89. Elliott BE, Meens JA, SenGupta SK, Louvard D, Arpin M. The membrane cytoskeletal crosslinker ezrin is required for metastasis of breast carcinoma cells. Breast cancer research : BCR. 2005;7:R365-73.

90. Makitie T, Carpen O, Vaheri A, Kivela T. Ezrin as a prognostic indicator and its relationship to tumor characteristics in uveal malignant melanoma. Investigative ophthalmology & visual science. 2001;42:2442-9.

91. Khanna C, Wan X, Bose S, Cassaday R, Olomu O, Mendoza A, et al. The membrane-cytoskeleton linker ezrin is necessary for osteosarcoma metastasis. Nature medicine. 2004;10:182-6.

92. Yu Y, Khan J, Khanna C, Helman L, Meltzer PS, Merlino G. Expression profiling identifies the cytoskeletal organizer ezrin and the developmental homeoprotein Six-1 as key metastatic regulators. Nature medicine. 2004;10:175-81.

93. Cui Y, Li T, Zhang D, Han J. Expression of Ezrin and phosphorylated Ezrin (pEzrin) in pancreatic ductal adenocarcinoma. Cancer investigation. 2010;28:242-7.

94. Hustinx SR, Fukushima N, Zahurak ML, Riall TS, Maitra A, Brosens L, et al. Expression and prognostic significance of 14-3-3sigma and ERM family protein expression in periampullary neoplasms. Cancer Biol Ther. 2005;4:596-601.

95. Oda Y, Aishima S, Morimatsu K, Hayashi A, Shindo K, Fujino M, et al. Differential ezrin and phosphorylated ezrin expression profiles between pancreatic intraepithelial neoplasia, intraductal papillary mucinous neoplasm, and invasive ductal carcinoma of the pancreas. Human pathology. 2013;44:1487-98.

96. Zhong ZQ, Song MM, He Y, Cheng S, Yuan HS. Knockdown of Ezrin by RNA interference reverses malignant behavior of human pancreatic cancer cells in vitro. Asian Pacific journal of cancer prevention : APJCP. 2012;13:3781-9.

97. Meng Y, Lu Z, Yu S, Zhang Q, Ma Y, Chen J. Ezrin promotes invasion and metastasis of pancreatic cancer cells. Journal of translational medicine. 2010;8:61.

98. Meerbrey KL, Hu G, Kessler JD, Roarty K, Li MZ, Fang JE, et al. The pINDUCER lentiviral toolkit for inducible RNA interference in vitro and in vivo. Proceedings of the National Academy of Sciences of the United States of America. 2011;108:3665-70.

99. Hu Y, Smyth GK. ELDA: extreme limiting dilution analysis for comparing depleted and enriched populations in stem cell and other assays. Journal of immunological methods. 2009;347:70-8.

100. Denham M, Huynh T, Dottori M, Allen G, Trounson A, Mollard R. Neural stem cells express non-neural markers during embryoid body coculture. Stem cells. 2006;24:918-27.

101. Bonello TT, Stehn JR, Gunning PW. New approaches to targeting the actin cytoskeleton for chemotherapy. Future medicinal chemistry. 2009;1:1311-31.

102. Maekawa M, Ishizaki T, Boku S, Watanabe N, Fujita A, Iwamatsu A, et al. Signaling from Rho to the actin cytoskeleton through protein kinases ROCK and LIM-kinase. Science. 1999;285:895-8.

103. Davies SP, Reddy H, Caivano M, Cohen P. Specificity and mechanism of action of some commonly used protein kinase inhibitors. The Biochemical journal. 2000;351:95-105.

104. Speck O, Hughes SC, Noren NK, Kulikauskas RM, Fehon RG. Moesin functions antagonistically to the Rho pathway to maintain epithelial integrity. Nature. 2003;421:83-7.

105. Matsumoto Y, Inden M, Tamura A, Hatano R, Tsukita S, Asano S. Ezrin mediates neuritogenesis via down-regulation of RhoA activity in cultured cortical neurons. PloS one. 2014;9:e105435.

106. Ohata H, Ishiguro T, Aihara Y, Sato A, Sakai H, Sekine S, et al. Induction of the stem-like cell regulator CD44 by Rho kinase inhibition contributes to the maintenance of colon cancer-initiating cells. Cancer research. 2012;72:5101-10.

107. Tilson SG, Haley EM, Triantafillu UL, Dozier DA, Langford CP, Gillespie GY, et al. ROCK Inhibition Facilitates In Vitro Expansion of Glioblastoma Stem-Like Cells. PloS one. 2015;10:e0132823.

108. Dard N, Louvet-Vallee S, Santa-Maria A, Maro B. Phosphorylation of ezrin on threonine T567 plays a crucial role during compaction in the mouse early embryo. Developmental biology. 2004;271:87-97.

109. Donatello S, Babina IS, Hazelwood LD, Hill AD, Nabi IR, Hopkins AM. Lipid raft association restricts CD44-ezrin interaction and promotion of breast cancer cell migration. The American journal of pathology. 2012;181:2172-87.

110. Yakovich AJ, Huang Q, Du J, Jiang B, Barnard JA. Vectorial TGFbeta signaling in polarized intestinal epithelial cells. Journal of cellular physiology. 2010;224:398-404.

111. Stehn JR, Haass NK, Bonello T, Desouza M, Kottyan G, Treutlein H, et al. A novel class of anticancer compounds targets the actin cytoskeleton in tumor cells. Cancer research. 2013;73:5169-82.

112. Celik H, Hong SH, Colon-Lopez DD, Han J, Kont YS, Minas TZ, et al. Identification of Novel Ezrin Inhibitors Targeting Metastatic Osteosarcoma by Screening Open Access Malaria Box. Molecular cancer therapeutics. 2015;14:2497-507.

113. Zhang GN, Liang Y, Zhou LJ, Chen SP, Chen G, Zhang TP, et al. Combination of salinomycin and gemcitabine eliminates pancreatic cancer cells. Cancer letters. 2011;313:137-44.

114. Feldmann G, Dhara S, Fendrich V, Bedja D, Beaty R, Mullendore M, et al. Blockade of hedgehog signaling inhibits pancreatic cancer invasion and metastases: a

new paradigm for combination therapy in solid cancers. Cancer research. 2007;67:2187-96.

115. Rajeshkumar NV, Rasheed ZA, Garcia-Garcia E, Lopez-Rios F, Fujiwara K, Matsui WH, et al. A combination of DR5 agonistic monoclonal antibody with gemcitabine targets pancreatic cancer stem cells and results in long-term disease control in human pancreatic cancer model. Molecular cancer therapeutics. 2010;9:2582-92.

116. Rooney P, Archer CW. The development of the perichondrium in the avian ulna. Journal of anatomy. 1992;181 (Pt 3):393-401.

117. Long F, Linsenmayer TF. Regulation of growth region cartilage proliferation and differentiation by perichondrium. Development. 1998;125:1067-73.

118. Cohen DM, Chen CS. Mechanical control of stem cell differentiation. StemBook. Cambridge (MA)2008.

119. Ozdemir BC, Pentcheva-Hoang T, Carstens JL, Zheng X, Wu CC, Simpson TR, et al. Depletion of carcinoma-associated fibroblasts and fibrosis induces immunosuppression and accelerates pancreas cancer with reduced survival. Cancer cell. 2014;25:719-34.

120. Rhim AD, Oberstein PE, Thomas DH, Mirek ET, Palermo CF, Sastra SA, et al. Stromal elements act to restrain, rather than support, pancreatic ductal adenocarcinoma. Cancer cell. 2014;25:735-47.

121. Balic A, Sorensen MD, Trabulo SM, Sainz B, Jr., Cioffi M, Vieira CR, et al. Chloroquine targets pancreatic cancer stem cells via inhibition of CXCR4 and hedgehog signaling. Molecular cancer therapeutics. 2014;13:1758-71.

122. Lonardo E, Cioffi M, Sancho P, Sanchez-Ripoll Y, Trabulo SM, Dorado J, et al. Metformin targets the metabolic achilles heel of human pancreatic cancer stem cells. PloS one. 2013;8:e76518.

CURRICULUM VITAE

Vesselin Ruslanov Penchev 03/20/2016

Educational History

Ph.D. expected	2016	Program in Cellular and Molecular Medi Mentor: William Matsui, MD	The Johns Hopkins University School of Medicine
B.A.	2007	Biology	Macalester College

Professional Experience

Junior Scientist	2007-2008	Stem Cell Institute, University of Minnesota, Minneapolis, MN

Awards and Honors

2013	Most Popular Poster at the Graduate Student Association Poster Presentation, The Johns Hopkins University School of Medicine
2010	Pollard Scholar in Graduate Immunology, The Johns Hopkins University School of Medicine
2007	O.T Walter Award for Promise of Success in the field of Medicine, Macalester College
2007	Science Tutor Recognition Award, Macalester College
2005-2007	Bill George International Scholarship, Macalester College
2005-2007	Kofi Annan International Scholarship, Macalester College

Peer-Reviewed Publications

- **Penchev** VR, Rasheed ZA, Maitra A, Matsui W. Heterogeneity and targeting of pancreatic cancer stem cells. Clin Cancer Res. 2012 Aug 15;18(16):
- Kopher RA, **Penchev** VR, Islam MS, Hill KL, Khosla S, Kaufman DS. Human embryonic stem cell-derived CD34+ cells function as MSC progenitor cells. Bone. 2010 Oct;47(4):718-28.
- Tian X, Hexum MK, **Penchev** VR, Taylor RJ, Shultz LD, Kaufman DS. Bioluminescent imaging demonstrates that transplanted human embryonic stem cell-derived CD34(+) cells preferentially develop into endothelial cells. Stem Cells. 2009 Nov;27(11):2675-85A

Published Abstracts

- Gocke CB**,** Wang Q, McMillan RH, **Penchev** VR, Sage J, Khavari PA, Matsui W. Inhibiting oncogenic RAS in multiple myeloma by targeting scaffold-ERK interactions. Blood 2014 Dec 6:124(21)

Teaching Activities

2010	Cell Physiology. Teaching assistant, The Johns Hopkins University School of Medicine
2010	Graduate Immunology. Co-organizer and leader of a supplementary lecture series, The Johns Hopkins University School of Medicine
2007	Molecular Neuroscience. Teaching assistant, Macalester College
2006-2007	Human Phyisiology. Teaching assistant, Macalester College
2006-2007	Cell Biology and Genetics II. Teaching assistant, Macalester College
2005	Cell Biology and Genetics I. Teaching assistant, Macalester College
2005	Calculus II. Teaching assistant, Macalester College
2004	Elementary Statistics. Teaching assistant, Macalester College

Mentoring

2013	Maya Thakkar, High school stutdent

2012-2013 Karly Raber, Undergraduate student
2010 Chris Murter, Undergraduate Student

Service and leadership

2010-2016 Junior Instructor, Baltimore Karate Club, Baltimore, MD
2012-2014 Patient Advocate, Health Leads at Bayview Emergency Department, Baltimore, MD